Geochemical modelling of CO2 dissolution in deep saline aquifers - the effects on brine composition

Tomljenović, Iva

UNIVERSITY OF ZAGREB

FACULTY OF MINING, GEOLOGY, AND PETROLEUM ENGINEERING

Graduate Study of Geology

GEOCHEMICAL MODELLING OF CO_2 DISSOLUTION IN DEEP SALINE AQUIFERS – THE EFFECTS ON BRINE COMPOSITION

Master´s Thesis

Iva Tomljenović

G-188

Zagreb, 2017.

Acknowledgement:

I would first like to thank my thesis supervisor prof.dr.sc. Bruno Saftić and other members of the advisory committee – doc.dr.sc. Vesnica Garašić, and doc.dr.sc. Iva Kolenković for their patience, advice and the overall help to finish my final thesis.

I would also like to thank dr.habil. Axel Liebscher and dr. Bernd Wiese for their mentorship and supervision at the GFZ during my internship stay and for giving me the opportunity to attend the ongoing project of the CO_2 storage in Ketzin, as well as giving me the permission to use the Ketzin´s data.

Also, many thanks to dr.sc. Krešimir Krimanić and Ms. Tihana Goričnik from INA – Industrija nafte d.d., for providing me the data which this thesis would not have been completed without.

A big thank to my family and friends for giving me a huge support and continuous encouragement throughout my studies.

This accomplishment would not have been possible without all of them.

Sveučilište u Zagrebu
Rudarsko-geološko-naftni fakultet

Diplomski rad

G – 188

GEOKEMIJSKO MODELIRANJE OTAPANJA CO_2 U DUBOKIM SLANIM VODONOSNICIMA – UTJECAJ NA KEMIJSKI SASTAV SLOJNE VODE

IVA TOMLJENOVIĆ

Diplomski rad je izrađen: Sveučilište u Zagrebu
Rudarsko-geološko-naftni fakultet
Zavod za geologiju i geološko inženjerstvo
Pierottijeva 6, 10 002 Zagreb

Sažetak

Geološko skladištenje ugljičnog dioksida u duboke slane vodonosnike jedna je od metoda smanjenja njegove koncentracije u atmosferi. Duboki slani vodonosnici su geološke formacije smještene na dubinama od 800 do 2500 m. U Hrvatskoj je istraživanje u fazi procjene kapaciteta, te su u prethodnim istraživanjima napravljene karte specifičnog kapaciteta uskladištenja za zapadni dio Savske depresije. Poljana pješčenjaci su izdvojeni kao potencijalna formacija za skladištenje. Budući da su u toj fazi poroznosti bile procijenjene u samo 20 bušotina, u ovome je radu pomoću statističkog programa NCSS, poroznost interpolirana na 60 bušotina. Potom je, zbog dostupnih podataka kemijske analize, odabrana bušotina Žu-249 za daljnje geokemijsko modeliranje otapanja ugljičnog dioksida u slojnoj vodi. Modeliranje je napravljeno u programu PHREEQC, metodom kemijske ravnoteže između slojne vode i otopljenog $CO_{2(g)}$. Ista stvar je napravljena za duboki slani vodonosnik u Ketzin-u, Njemačka. Za model Ketzin korišteni su podatci o sastavu slojne vode koja je analizirana prije utiskivanja, 2008. godine, i 2014. godine, šest godina nakon početka utiskivanja. Na kraju su svi modeli uspoređeni kako bi se dobila opća slika o sigurnosti uskladištenja $CO_{2(g)}$ u duboke slane vodonosnike s obzirom na mineraloški različite formacije, različite dubine zalijeganja, temperature, tlakove i salinitete vode kao ključne parametere. Zaključeno je da je relativno sigurno skladištiti $CO_{2(g)}$ u duboke slane vodonosnike. $CO_{2(g)}$ mijenja pH vode, te u takvom promijenjenom sistemu, novi minerali precipitiraju i $CO_{2(g)}$ se polako odstranjuje iz vodonosnika.

Ključne riječi: ugljični dioksid, geološko skladištenje CO_2, Savska depresija, pješčenjaci Poljana, duboki slani vodonosnik, multipla regresija, Žutica, Ketzin, PHREEQC

Završni rad sadrži: 58 stranica, 28 slika, 5 tablica, 8 priloga, 36 referenci
Jezik izvornika: engleski
Diplomski rad pohranjen: Knjižnica Rudarsko-geološko-naftnog fakulteta
Pierottijeva 6, Zagreb
Voditelj: Izv. prof. dr. sc. Bruno Saftić
Ocjenjivači: 1. Izv. prof. dr. sc. Bruno Saftić
2. Doc. dr. sc. Vesnica Garašić
3. Doc. dr. sc. Iva Kolenković Močilac

Datum obrane: 21.07.2017

University of Zagreb
Faculty of Mining, Geology, and Petroleum Engineering

Master´s Thesis

G-188

GEOCHEMICAL MODELLING OF CO_2 DISSOLUTION IN DEEP SALINE AQUIFERS – THE EFFECTS ON BRINE COMPOSITION

Iva Tomljenović

Thesis completed in: University of Zagreb
Faculty of Mining, Geology and Petroleum Engineering
Department of Geology and Geological Engineering
Pierottijeva 6, 10 002 Zagreb

Abstract

Geological storage of carbon dioxide in deep saline aquifers is one of the methods of reducing its concentration in the atmosphere. Deep saline aquifers are geological formations located at depths that range from 800 to 2500 metres. In Croatia, a research has recently been conducted based on capacity estimations. Therein created geological maps of specific storage capacities in the Western part of Sava depression are confined to the Poljana sandstones that were singled out as a potential storage unit. Since the porosity had been measured in only 20 wells, in this study, this parameter was extrapolated to 60 wells, using NCSS statistical software. After that, due to the only available data of the water composition from the observed area, well Žu-249 has been selected for further geochemical modelling of $CO_{2(g)}$ dissolution in brines. The modelling has been performed with the PHREEQC program implementing chemical equilibrium between formation water and dissolved $CO_{2(g)}$. The same model has been created for deep saline aquifer in Ketzin, Germany. The Ketzin models have been made with the available data from water analysis prior the injection, in 2008, and in 2014, six years after the injection had started. Finally, all the models were compared to obtain a general picture of the CO_2 storage efficiency and safetey due to mineralogically different formations, different depths, temperatures, pressures and salinities as the key parameters. The most important findings are that it is relatively safe to store $CO_{2(g)}$ in this type of aquifers. $CO_{2(g)}$ changes pH of water and under the new circumstances certain minerals precipitate and $CO_{2(g)}$ is slowly being removed from the brine.

Keywords: carbon dioxide, geological CO_2 storage, Sava depression, Poljana sandstones, deep saline aquifer, multiple regression, Žutica, Ketzin, PHREEQC

Thesis contains: 58 pages, 28 figures, 5 tables, 8 enclosures, 36 references
Original in: English
Thesis deposited in: Library of Faculty of Mining, Geology, and Petroleum Engineering
Pierottijeva 6, Zagreb
Supervisor: PhD Bruno Saftić, Associate Professor
Technical support and assistance:
Reviewers: 1. PhD Bruno Saftić, Assoc.Professor
2. PhD Vesnica Garašić, Assist. Professor
3. PhD Iva Kolenković Močilac, Assist. Professor
Date of defence: 21.07.2017

Table of Contents

1 INTRODUCTION 1
2 GEOLOGICAL STORAGE 3
2.1 Geological Formations 3
2.2 CO_2 Injection and Flow 4
3 GEOLOGY OF THE KETZIN AND ŽUTICA STORAGE SITES 6
3.1 Ketzin 6
3.2 Sandstone Reservoirs in the Western Part of Sava Depression 8
4 OVERVIEW OF STORAGE CAPACITY ESTIMATIONS IN SAVA DEPRESSION 11
4.1 Methodology 11
4.2 Effective Thickness of the Deep Saline Aquifer Poljana 12
4.3 Pressure 13
4.4 Temperature 14
4.5 Porosity 15
5 WATER CHEMISTRY 16
5.1 Elements and Species in Water 16
5.2 Solution Thermodynamics – Ionic Strength 17
5.3 Calculation of Activity Coefficients 18
5.4 Carbonate Equilibria 19
6 PHREEQC PROGRAM CALCULATIONS 21
6.1 Application to Reservoir Models 21
6.2 Calculation of saturation indices 23
7 PHREEQC MODELS OF THE REGIONAL DSA POLJANA AND THE KETZIN STORAGE SITE 24
7.1 Deep Saline Aquifer Poljana 24
7.1.1 Statistical Analysis of Porosity Distribution 24
7.1.2 Multiple Regression 25
7.1.3 Input Data – the Žutica well 27
7.1.4 Results – the Žutica well 28
7.2 Ketzin 31
7.2.1 Back-production Test 31
7.2.2 Input Data – Ketzin 32
7.2.3 Results – Ketzin 34
8 DISCUSSION 40
9 CONCLUSION 43

10 REFERENCES 45
10.1 Published 45
10.2 Archived documents 49
10.3 Web sources 49

List of Figures

Figure 2-1 Illustration of CO2 injection into deep saline formations and its behaviour in subsurface. .. 3
Figure 2-2 Increasing storage security over time through various trapping mechanism (IPCC, 2005). . 5
Figure 3-1 Roskow-Ketzin double anticline (NORDEN et al., 2013). 6
Figure 3-2 During the back-production test water has been pumped out from the well Ktzi-201 7
Figure 3-3 Map of the Western part of Sava Depression with the study area marked with the red line. 8
Figure 3-4 The largest stationary sources of CO2, deep saline aquifers, depleted oil and gas fields, and regional pipeline infrastructure in Croatia (SAFTIĆ et al., 2008). 9
Figure 3-5 Lithostratigraphic scheme of Neogene strata in Sava Depression (from KOLENKOVIĆ, 2012, after ŠIMON, 1970). 10
Figure 4-1 Results of the porosity evaluation for the well Žu-249DU (KOLENKOVIĆ, 2012; analysis and composite chart have been done by Zvonko Jeras, grad.ing.geol). 12
Figure 4-2 Diagram of CO2 density (VULIN 2010, using the equation from SPAN & WAGNER, 1996). 13
Figure 5-1 Deviation of solution from the ideal; Ketzin´s brine. 17
Figure 5-2 Ionic strength of the different types of natural waters (left) and salinities expressed as total dissolved solids (TDS) for different types of natural waters (right). 18
Figure 5-3 A speciation diagram for the carbonic acid system in seawater as a function of pH. 20
Figure 6-1 Required steps for obtaining a model of an aqueous system. 21
Figure 6-2 Equilibrium model in the PHREEQC simulation. A free CO2(g) is a system boundary of the solution. 22
Figure 6-3 Dense CO2(g) migrating upwards (light blue bubbles) dissolving and reacting with the grains of the rock, leading to precipitation of minerals on the grain boundaries (white) (CO2GeoNet, 2007). 23
Figure 7-1 3D scatter plot of measured porosity vs effective thickness. Green coloured is a regression plane (location of deep wells taken from KOLENKOVIĆ, 2012). 24
Figure 7-2 Contour plot of measured porosity values vs. mean depth and effective thickness of DSA Poljana (SAFTIĆ et al., 2015). 25
Figure 7-3 Residuals of measured porosity. 26
Figure 7-4 Histogram of residuals of measured porosity. 26
Figure 7-5 Transformation of the brine analysed in the laboratory to the reservoir conditions – Žutica well, 15.10.2014. 30
Figure 7-6 Third step of the simulation with the PHREEQC database. 30
Figure 7-7 Cumulative mass of produced fluids during the back-production test (data from water analyses of PWU and GFZ). 31
Figure 7-8 Variation of bottomhole pressure during the back-production test (WIESE B., 2014). 32
Figure 7-9 Sodium and iron concentration over cumulative mass of produced fluids (Data taken from the water analyses of GFZ and PWU). 33
Figure 7-10 Saturation indices of mineral phases for three steps of batch-reactions. 36
Figure 7-11 The average values of concentration of ions in mg/l that have been analysed during the pre-injection and back-production test. 37
Figure 7-12 Saturation indices. 39
Figure 8-1 Plot of CO2(g) – Calcite-anhydrite stability at different temperature (Ketzin back-production 16.10.2014; pitzer.dat). 41

List of Tables

Table 5-1 Carbonate equilibrium (STUMM & MORGAN, 1996). 20
Table 7-1 Certain parameters at the mean depth of the DSA Poljana in the location of well Žu-249D taken from KOLENKOVIĆ (2012). 28
Table 7-2 Žutica – parameters. 29
Table 7-3 Physical parameters – back-production test – October 16, 2014. 35
Table 7-4 Physical parameters. 38

List of Appendices

Appendix 1 NCSS multiple regression analysis 50
Appendix 2 Žu-249 – Water chemistry 52
Appendix 3 Percent errors in charge balance – Žu-246 53
Appendix 4 Žutica 249 – PHREEQC simulation 54
Appendix 5 Ketzin – PHREEQC simulation – First day of back-production test 55
Appendix 6 Ketzin – PHREEQC – The last day of back-production test 56
Appendix 7 Ketzin – PHREEQC simulation – Pre-injection data 57
Appendix 8 Chemical formulas of some minerals from the simulation 58

LIST OFABBREVIATIONS:

CCS – carbon capture and storage

CGS – CO_2 geological storage

d.s.a. - deep saline aquifer

LIST OF SYMBOLS:

pH - a measure of the activity of hydrogen ions

pe - a measure of the tendency of an solution to accept an electron

A - a surface of regional deep saline aquifer

M_{CO_2} - total storage capacity

$M_{CO_{2spec}}$ - specific storage capacity

S_{eff} - coefficient of storage effectiveness

ρ_{CO_2} - partial pressure of $CO_{2(g)}$

Φ - porosity

p - pressure

γ - activity coefficient

a - activity

m_i - molality or molal concentration (mol/kg)

n - number of moles

I - ionic strength

e - residuals in multiple regression analysis

y - an observed value

ŷ - a predicted value

c_i - molar concentration (mol/l)

z - electrical charge

SI - saturation index

log IAP - logarithm of ion activity product (activities in the water)

log K - logarithm of equilibrium constant (activities at equilibrium)

f - fugacity

φ - fugacity coefficient

1 INTRODUCTION

According to the International Energy Agency (IEA) publication Energy Technology Perspectives 2010 (ETP 2010), in the absence of new energy policies or supply constraints, energy-related carbon dioxide emissions in 2050 will be twice 2007 levels. The main reason is the increased combustion of fossil fuels. It is necessary to establish CO_2 atmospheric concentration below 450 parts per million and limit the long-term global mean temperature rise to less than 2.0°C above the pre-industrial levels.

Carbon dioxide geological storage (CGS) in suitable subsurface storage objects is one of the most acceptable and safety options for stabilisation of the atmospheric greenhouse gas concentrations. Carbon dioxide is firstly separated from the industrial and energy-related sources, then transported to a storage site where is being isolated from the atmosphere on the long-term basis by injecting it into suitable geological formation.

Method discussed in this thesis is CO_2 storage in deep saline aquifers (DSA). The other potential storage methods are geological storage in other geological formations such as depleted oil and gas fields or coal beds, ocean storage (direct release into the ocean water column or onto the deep seafloor), industrial fixation of CO_2 into inorganic carbonates, and disposal in basalts and lakes beneath ice caps.

Large point sources of CO_2 are large fossil fuel or biomass energy facilities, major CO_2-emitting industries, natural gas-recovering facilities, synthetic fuel plants and fossil fuel-based hydrogen production plants (IPCC, 2005).

Even though Croatia has low CO_2 emissions nowadays, it may not have in the future, and Carbon dioxide capture and storage policy (CCS) and regulations can change into that each country must make a contribution by having its own CCS facility. Following the regulations, detailed maps of storage capacity in the Western part of Sava depression have been made together with the initial thermodynamic and petrographic modelling. The primary target for CO_2 injection are Poljana sandstones and the primary objectives of the research have been the determination of porosity, reservoir thickness, depth, cap rock, temperature and pressure distribution in that area (KOLENKOVIĆ, 2012).

This thesis comprises most of the mentioned parameters which are essential for CCS, so it gives a broader view on the scale of a project comparing considered storage site in the Western Sava depression in Croatia with the Ketzin in Germany, onshore storage site, which is in the closure phase. However, the emphasis of this study is on the water chemistry of the Ketzin site, and Poljana sandstones of the Žutica field, Western Sava depression, Croatia. Moreover, it includes some of the statistical analyses of the porosity distribution of Poljana sandstones in the Western Sava depression. This was done in order to connect the data on formation water composition from the Žu-249 well with the storage capacity estimations in a broader area.

As there is a possibility of $CO_{2(g)}$ leakage into the shallower aquifers (main water supplies for households) or of causing increased dissolution of the carbonate cemented reservoir rocks, the main concern is the storage safety. Thus, $CO_{2(g)}$ dissolution has been modelled in the PHREEQC program for both aquifers and the results are compared concerning different subsurface environments.

2 GEOLOGICAL STORAGE

2.1 Geological Formations

Transported and deposited mineral and rock grains, organic material, and secondary minerals are the main constituents of geological sedimentary rock formations. The porous space between grains, open cavities and fractures are occupied by fluid which is in the most cases water. Basins suitable for CO_2 storage must have thick accumulations of sediments, the structure has to be simple, e.g. gently dipped anticline without many faults, the formations need to have medium to high permeability and must be saturated with saline water. Also, there must be an extensive cover of low-permeability rocks, pelitic sediments (***Figure 2-1***). Basins that are too shallow or if their main constituents are low-permeability or poorly confined rocks are not suitable for CO_2 storage (IPCC, 2005).

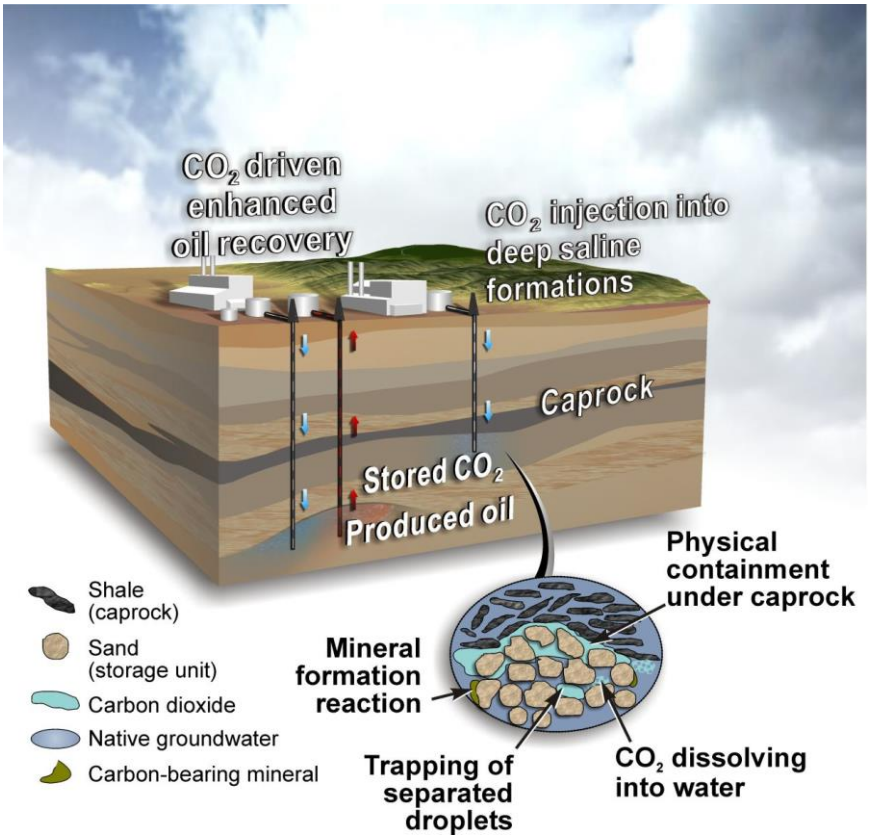

Figure 2-1 *Illustration of CO2 injection into deep saline formations and its behaviour in subsurface.*

(http://www.dbstephens.com/Geologic_Carbon_Sequestration.aspx)

At depths greater than 800 m, various physical and geochemical trapping mechanisms prevent stored CO_2 from migration to the surface. The buoyant plume of injected

CO_2migrates upwards unevenly due to permeability heterogeneities – intersections of low-permeability layers. Impermeable to relatively impermeable cap rocks cause lateral migration of the injected CO_2 which is then infilling any stratigraphic or structural trap on its way (IPCC, 2005).

CO_2 reaches a supercritical state at the depth of approximately 800 m, so that is the point where the density starts increasing rapidly. In places of the average geothermal gradients and hydrostatic pressures, at depths greater than 1.5 km, the density and specific volume become nearly constant. Without the presence of cap rock which is an essential trapping mechanism, CO_2 cannot be stored.

The storage can be combined with the Enhanced Oil Recovery (EOR) which leads to greater revenues from the oil and gas recoveries (IPCC, 2005). Geological storage projects are divided into several sections including well-drilling technology, injection technology, computer simulations – static and dynamic geological models and monitoring methods such as Electrical Resistivity Tomography (ERT), which are detecting CO_2 migration through layers.

2.2 CO_2 Injection and Flow

$CO_{2(g)}$ is injected into deep geological formations by pumping fluids down into a well end entering the permeable formation through the perforation hole (tunnel) or permeable screen which is usually 10–100 m thick. The injection increases pressure near the well so in that way CO_2 can enter the pore spaces initially occupied by the in situ formation fluids. The pressure raise mostly depends on the rates of injection, thickness of the permeable formation and their permeability (IPCC, 2005). Several transport mechanism control the distribution of CO_2 plume. One of them is fluid flow which is caused by pressure gradient, that is a result of the injection, or by natural hydraulic gradients. Buoyancy appears as a result of density differences between CO_2 and the formation fluids. There is also a diffusion process (movement from an area of high concentration to an area of low concentration), dispersion, permeability of rocks, and mineralisation after dissolution of CO_2 in water (IPCC, 2005).

Injected CO_2 can dissolve in or mix with the in-situ fluids and react with the rocks (mineral grains). Usually, all of these processes are present in one storage site. These processes are commonly called ″trapping mechanisms″. At first, CO_2 is trapped under an

impermeable layer - cap rock which is called structural trapping, a few percent of CO_2 is usually trapped inside the pores of formation rocks in a way that are being disconnected from the rest of plume during its migration to the top of the reservoir (residual trapping), some CO_2 dissolves in water and as the water with CO_2 is heavier, it sinks to the bottom of the reservoir (solubility trapping). Dissolved CO_2 in water forms a weak carbonic acid which reacts with the rock forming minerals and under new conditions some minerals dissolve while the other precipitate (mineral trapping) ***(Figure 2-2)***. Each mechanism depends on many geological and aqueous characteristics, and the timing of each process cannot be generalised. The final result is a mineral trapping and it is suggested that in that phase CO_2 is not a threat for the environment.

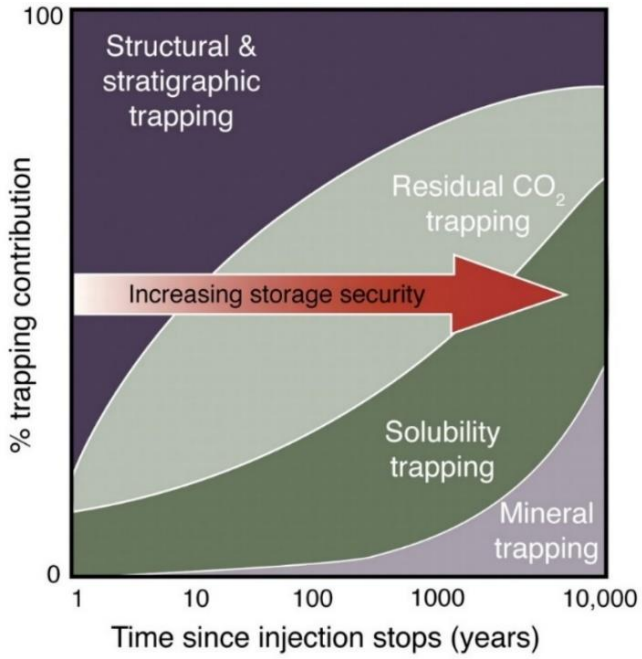

Figure 2-2 *Increasing storage security over time through various trapping mechanism (IPCC, 2005).*

According to DOUGHTY et al. (2001), in systems with slowly flowing water, reservoir-scale numerical simulations show that, over tens of years, a significant amount, up to 30% of the injected CO_2, will dissolve in formation water as it migrates through the formation. Basin-scale simulations show that the entire CO_2 plume dissolves in formation over centuries (IPCC, 2005).

3 GEOLOGY OF THE KETZIN AND ŽUTICA STORAGE SITES

3.1 Ketzin

The Ketzin locality, Brandenburg (Germany) is the first European onshore CO_2 storage site in the saline aquifer. The pilot storage site is situated in the Northeast German Basin around 25 km west of Berlin (***Figure 3-1***) and it is located on the south-eastern flank of the gently dipping Roskow-Ketzin double anticline (NORDEN et al., 2010)**.**

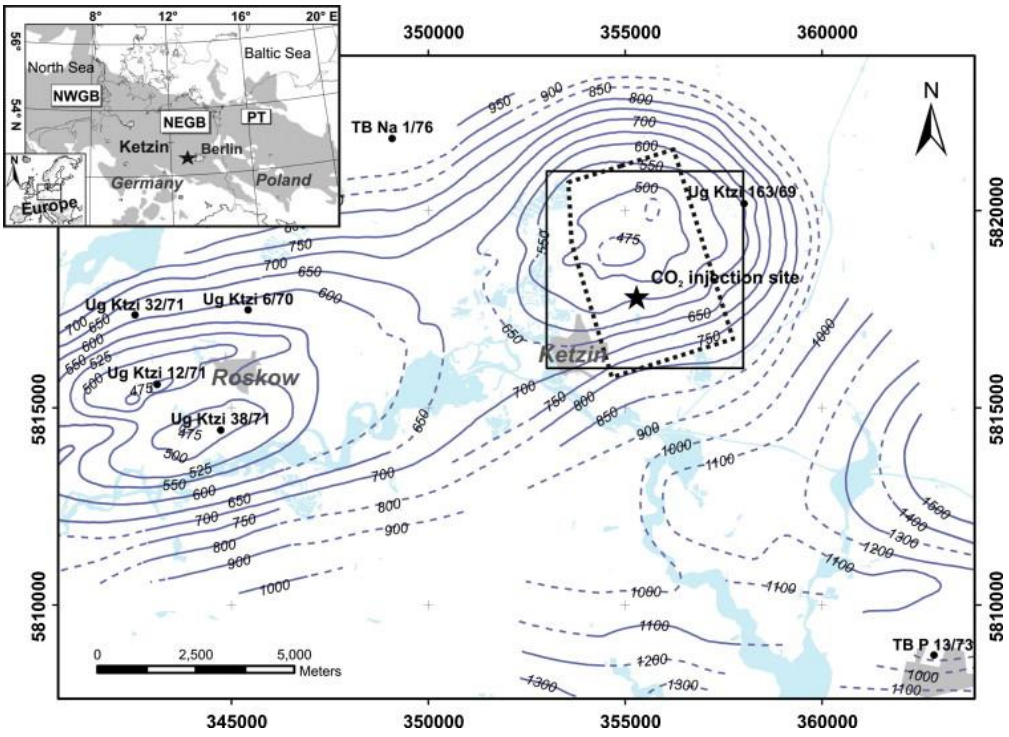

Figure 3-1 *Roskow-Ketzin double anticline (NORDEN et al., 2013).*

In summer of 2007, one injection well (Ktzi 201) and two observation wells (Ktzi 200 and 202) had been drilled to depths of 750–800 m. According to SCHILLING et al. (2009), the wells are about 50 to 110 m away from each other and arranged in a triangular shape (***Figure 3-2***).

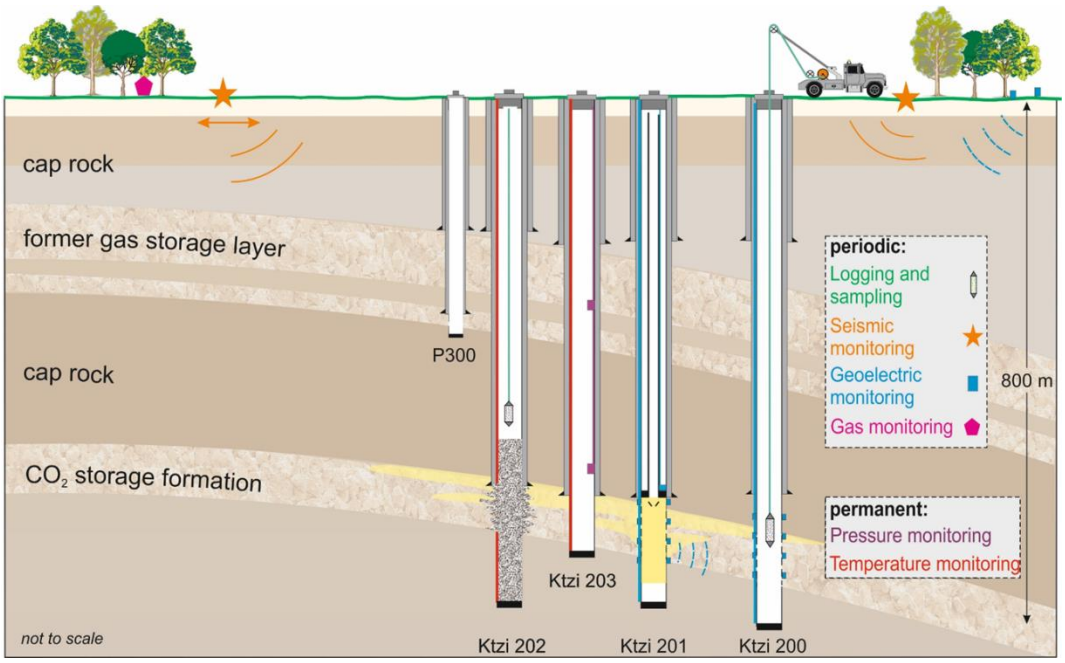

Figure 3-2 *During the back-production test water has been pumped out from the well Ktzi-201*

(www.co2ketzin.de)

Since June 2008 to August 2013 a total of 67,271 t of a food-grade CO_2 with a purity of >99.9vol% CO_2 has been injected into sandstone horizon of the Upper Triassic (Middle Keuper) Stuttgart Formation on the south-eastern flank of the anticline. At Ketzin, the Stuttgart Formation is 75–80 m thick, while the main reservoir horizon is only 9–20 m thick (NORDEN et al., 2010).

The Stuttgart Formation was deposited in a fluvial system, where the sandstone horizons represent river channel deposits. According to FORSTER et al. (2010), this type of depositional environment causes a high lateral and vertical heterogeneity between, but also within the individual sandstone horizons. The sandstones are mostly fine-grained with a general modal composition of 35-39 % quartz, ~ 20% feldspar, 13-18% illite, ~ 5% analcime, up to 10% anhydrite, plus minor variable amounts of mica, dolomite, hematite, pyrite and chlorite. Their porosity varies between 5% and >35%, and permeability is between 0.02 and > 5000 mD (NORDEN et al., 2010).

The reservoir horizon is at the depth of 625-650 m and the initial reservoir conditions were approximately 33°C and 62 bar, which increased to approximately 33°C and 75 bar during ongoing injection of CO_2. The reservoir conditions correspond to a CO_2 density of ~ 0.3 g/cm^3 (SPAN & WAGNER, 1996), which is lower than the CO_2 density of ~ 0.8 g/cm^3 targeted for future industrial-scale storage sites (FISCHER, 2013).

3.2 Sandstone Reservoirs in the Western Part of Sava Depression

The Sava depression is the large subsided structural unit that stretches in SE direction roughly from Zagreb all the way to the south of the Slavonian mountains. Its western part is shown in ***Figure 3-3*** where the area chosen for detailed study is highlighted. Several oil and gas fields were discovered and exploited in this area. The most numerous reservoirs are characterized by intergranular porosity and hydrocarbons were accumulated in the Upper Miocene sandstone-marlstone sequence.

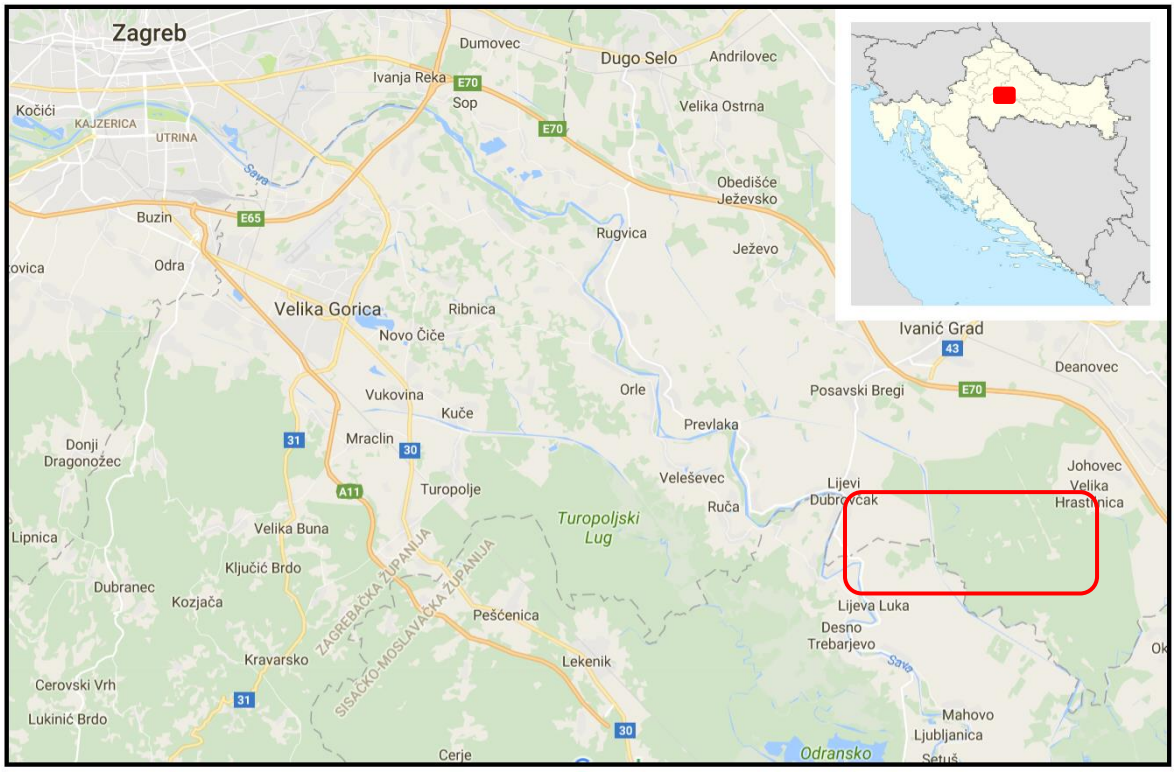

Figure 3-3 *Map of the Western part of Sava Depression with the study area marked with the red line.*

Considered storage site is located in the central part of Croatia, and one benefit is that four thermal power plants and one natural gas processing plant, all with large yearly emissions of CO_2, are located less than 100 km from this area (***Figure 3-4***). It is also convenient that there is a dense pipeline infrastructure that was built for the surrounding oil and gas fields which would greatly facilitate planning of the transport for CO_2 (SAFTIĆ et al. 2008).

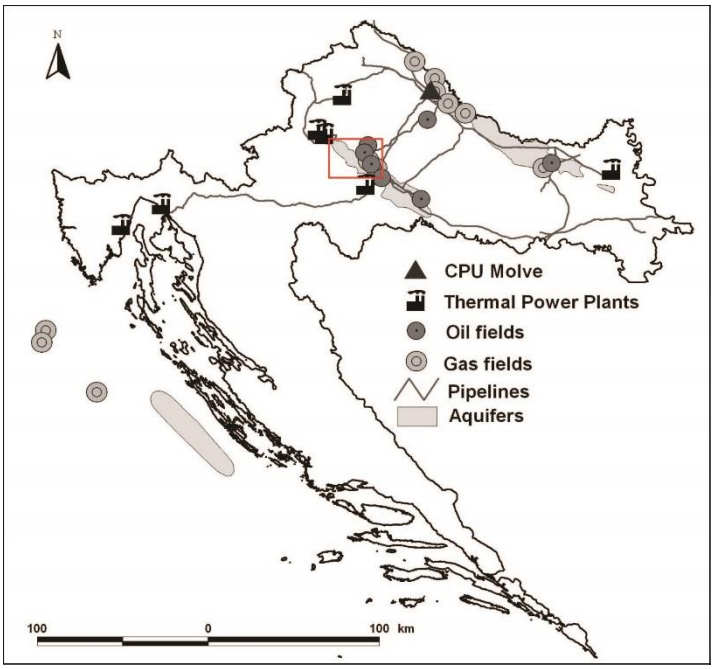

Figure 3-4 *The largest stationary sources of CO2, deep saline aquifers, depleted oil and gas fields, and regional pipeline infrastructure in Croatia (SAFTIĆ et al., 2008).*

According to TADEJ & KRIZMANIĆ (1996), the distribution and geometry of the Upper Miocene sandstone bodies were strongly influenced by depositional paleo-environment, deltaic and shelf processes (***Figure 3-5***). For example, Iva sandstones from the Ivanić oil field are deposited on the shallow indented shelf. ¸SAFTIĆ et al. (1995) interpreted Poljana sandstones of the Žutica field as a dendritic paleo-drainage pattern characterized by the three major channel sandstone bodies. Sand bodies in the Sava depression have thicknesses from few meters up to several hundred meters (TADEJ et al., 1996).

According to TADEJ et al. (1996), the Upper Miocene sandstone reservoirs in the Sava depression are fine to medium grained and mostly well sorted. Major components of sandstones are quartz (40-50%), rocks fragments (15-25%), micas (10-15%), feldspars (5-10%) and cement (5-20%). Micas, altered feldspars, chlorite, chert, quartzite, dolomite and mica-schist rock fragments have been found as minor constituents. Secondary intergranular pores are mostly infilled with Fe-rich carbonate cement (Fe-calcite, Fe-dolomite). Variations of clay mineral content has been determined with the SEM microscopy. It has been found that both illite and kaolinite were infilling pores while illite was also present in the form of coatings (TADEJ et al., 1996).

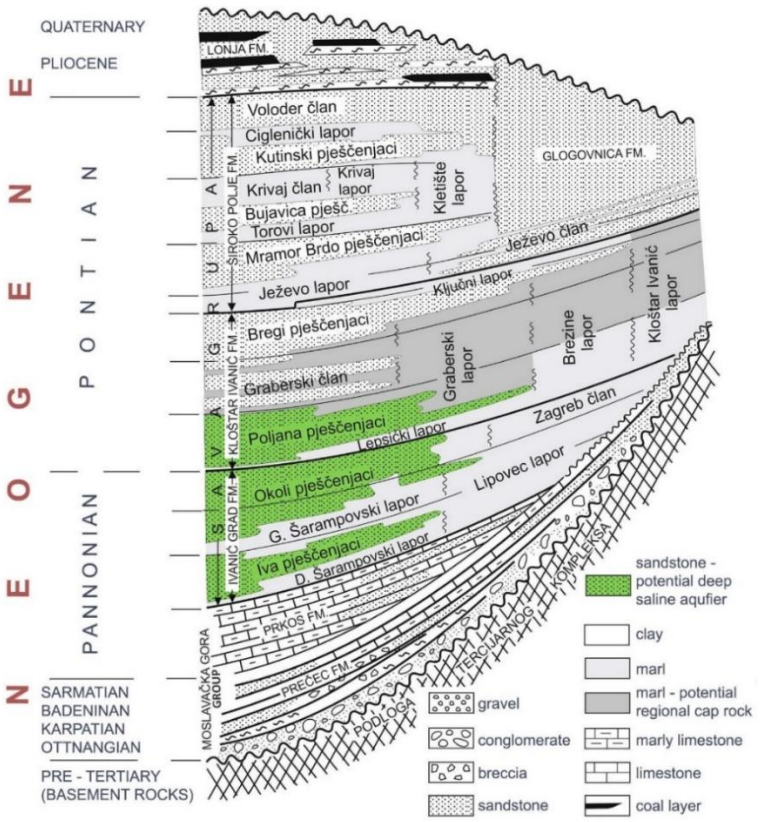

Figure 3-5 *Lithostratigraphic scheme of Neogene strata in Sava Depression (from KOLENKOVIĆ, 2012, after ŠIMON, 1970).*

Porosity has been reduced through compaction and cementation processes. According to TADEJ et al. (1996) variation in porosity and permeability at depth is a function of sedimentary conditions, distribution of the sandstone bodies, cementation and dissolution. TADEJ et al. (1996) noted that sandstone reservoirs can be divided into three groups differing in cementation and porosity-permeability patterns:

1) sandstones with less than 5% cement, and with high porosity (23-33%) and permeability from 30 to 380 x $10^{\wedge-3}$ μm^2;
2) sandstones with 5–10% cement and average porosity of 19-30% and permeability from 7 to 105 x 10^{-3} μm^2;
3) highly cemented (up to 20% cement) which are less abundant.

Pelitic sediments are mostly marls and calcitic marls (TADEJ &KRIZMANIĆ, 1995), which are effective cap rocks rocks for hydrocarbons.

4 OVERVIEW OF STORAGE CAPACITY ESTIMATIONS IN SAVA DEPRESSION

4.1 Methodology

Storage capacity can be calculated with the following equation (US Department of Energy- US DOE, 2007, 2010):

$$MCO_2 = A\, h\, \phi\, pCO_2 S_{eff} \quad (4\text{-}1)$$

where MCO_2[t] is a storage capacity, A [m^2] is surface of regional deep saline aquifer, h [m] is average effective thickness of a deep saline aquifer, ϕ is average porosity, ρ [kg/m^3] is CO_2 density in subsurface conditions and S_{eff} is a coefficient of storage effectiveness which characterizes the fraction of pore space that is possible to infill with CO_2.

All of the estimates are just approximations and proper methodology to be implemented in each basin should match the specific subsurface conditions, structure, and available data. The advantages of this methodology are its simplicity and possibility to be used with a limited data set. However, the results cannot be the basis for a delineation of the local CO_2 storage site. S_{eff} had been derived for the sedimentary basins in USA and Canada, so in the absence of a better solution, it was used for the storage capacity estimations in Europe (FP6 EU GeoCapacity, 2009). The conservative value of 2% for S_{eff} is taken for this purpose.

Beside the total storage capacity, it is possible to estimate the specific storage capacity, which is defined as a storage capacity of the deep saline aquifer per square kilometre:

$$MCO_{2,spec} = \frac{M(CO_2)}{A} \quad (4\text{-}2)$$

where $MCO_{2,spec}$ [t/km^2] is a specific storage capacity of the deep saline aquifer, $M(CO_2)$ is a total storage capacity of the regional aquifer, and A [km^2] is a surface area of the investigated aquifer block.

4.2 Effective Thickness of the Deep Saline Aquifer Poljana

The aquifer itself is a composite unit, it represents a sum of one to seven sandstone layers, depending on the location. The greatest thicknesses are in the central and the deepest parts of the depression. The upper vertical boundary of DSA Poljana is the depth of 800 m, while the maximum depth for storage is 2500 m. According to KOLENKOVIĆ (2012), in the area where sandstones are found lying at depth between these two values, the mean depth of Poljana sandstone has been calculated. On the well log-diagram (***Figure 4-1)*** is shown the depth of Poljana sandstones at the location of Žu-249D together with the porosity of sandstones. Depths greater than 2500 m were excluded due to economic reasons. The increased formation pressures in greater depths may be an obstacle.

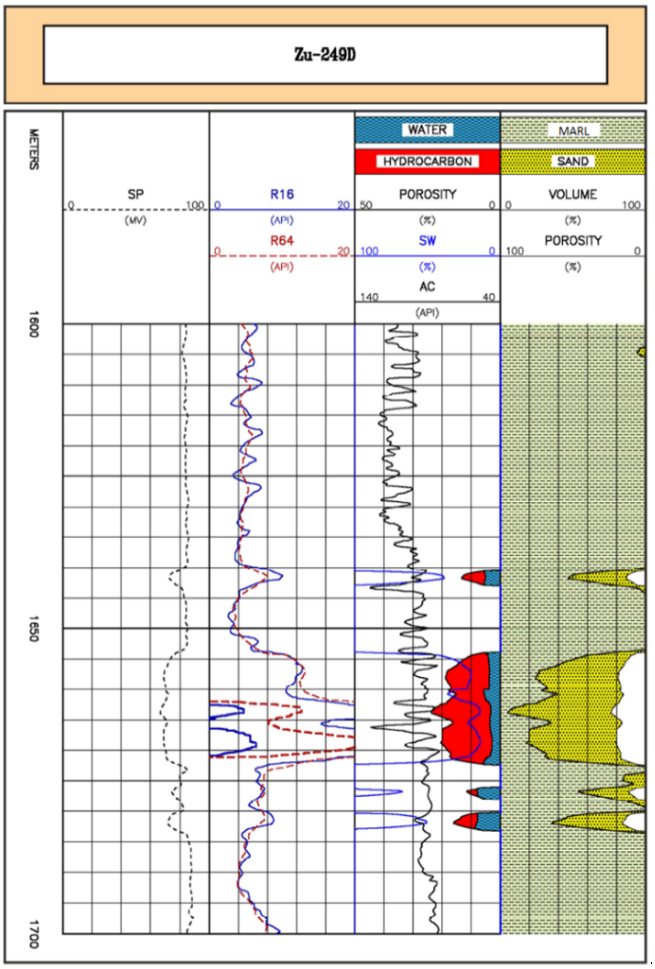

Figure 4-1 *Results of the porosity evaluation for the well Žu-249DU (KOLENKOVIĆ, 2012; analysis and composite chart have been done by Zvonko Jeras, grad.ing.geol).*

4.3 Pressure

CO_2 must be injected to formations with initial formation pressure higher than 73.8 bar, in order for it to be in supercritical state. The pressure of ″supercritical″ CO_2 is a function of the difference in CO_2 density and density of formation water, given by the equation:

$$p\ CO_2 = (\rho_w - \rho\ CO_2)\ g\ h \quad (4\text{-}3)$$

where p is pressure [bar], ρ_w density of porous water [kg/m^3], ρCO_2 [kg/m^3] is a density of CO_2, g standard gravity [m/s^2], and h is the elevation of the CO_2 plume.

CO_2 density is higher under the higher pressure ***(Figure 4-2)***, so the capacity is then enlarged. There is also an upper limit, too high injection pressure may cause rock fractures and therefore loss of the cap rock integrity (KOLENKOVIĆ, 2012).

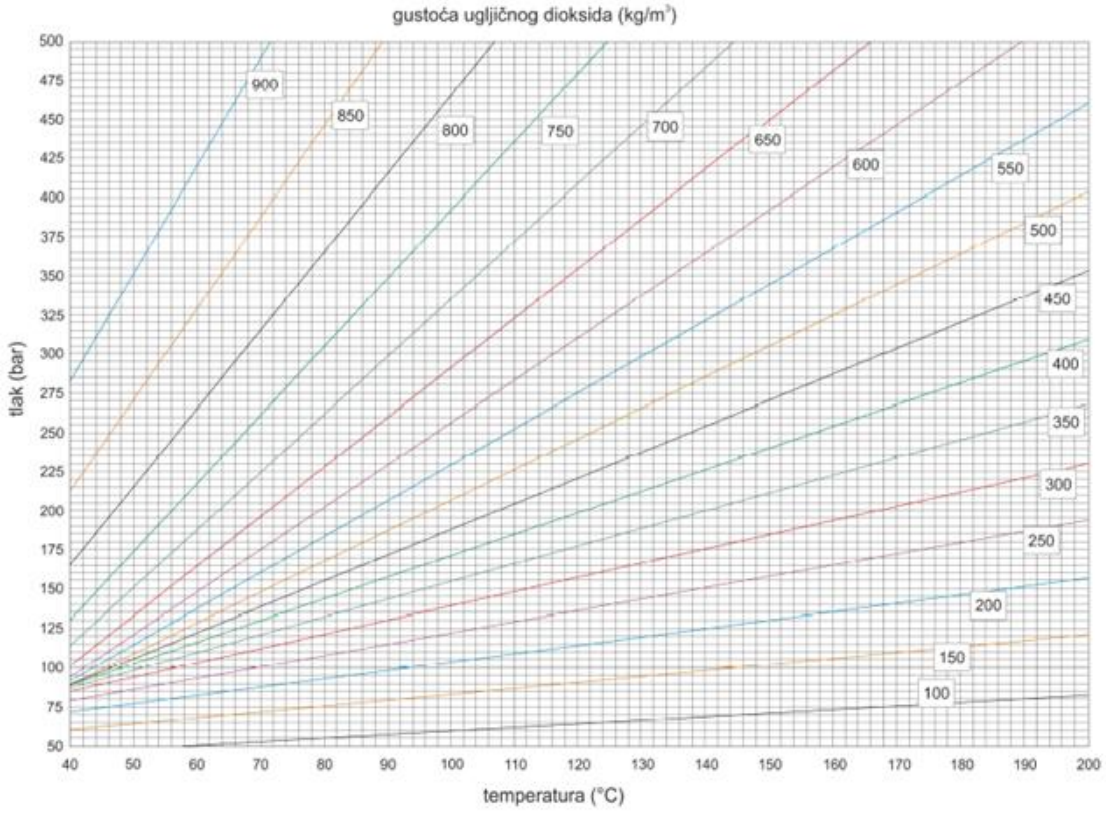

Figure 4-2 *Diagram of CO2 density (VULIN 2010, using the equation from SPAN & WAGNER, 1996).*

The hydrostatic pressure of formation water in Poljana sandstones was estimated from the reports of Total Drilling Control (TDC) measurements in the deep exploration wells

(KOLENKOVIĆ, 2012). The hydrostatic gradient in the observed area is approximately 10 bar/100 m, so a pressure at the mean depth of the DSA is calculated with the equation:

$$p = G_h d_{mean}/100 \quad (4\text{-}4)$$

where p is pressure [bar] at the mean depth d_{mean} [m], and G_h is hydrostatic pressure gradient [bar/100 m].

4.4 Temperature

According to KOLENKOVIĆ (2012), temperatures have been calculated from the map of thermal gradient which has been constructed from multiple temperature measurements in 17 wells. Even though bottomhole temperature measurements were available from 100 wells, thermal gradients have only been determined from the wellbores from which static temperature could be calculated based on several results of temperature measurements for which the exact time of measurement, after the cessation of drill-fluid circulation, has been recorded. For each well a temperature at the mean depth of the DSA has been calculated with the following equation:

$$T_{mean} = T_{mean\ annual} + \frac{Gt\ d_{mean}}{100} \quad (4\text{-}5)$$

where $T_{mean\ annual}$ is mean annual temperature [°C], Gt is geothermal gradient [°C/100], and d_{mean} is mean depth of deep saline aquifer.

Mean annual temperature for the study area is considered to be 10.7°C, according to the data from meteorological station Maksimir, Zagreb.

Pannonian basin has a quite high-temperature gradient, and within the investigated area the temperature at the depth of 800 m is higher than the critical temperature for CO_2 storage of 31°C (KOLENKOVIĆ, 2012). At the critical temperature and pressure, $CO_{2(g)}$ is expanding like a gas, but has the density of a fluid.

4.5 Porosity

Porosity is one of the most important parameters for regional storage capacity estimations. The porosity was measured in 20 wells using standard well logs (acoustic, density and neutron logging) by INA d.d.. In the laboratory of INA d.d., porosities have only been measured on a few core samples and that data has not been used for this research. The mean porosities of the DSA Poljana were calculated for 20 locations (KOLENKOVIĆ, 2012), and 18 of them have been used as the input data for statistical analyses. The sandstones are pinching out into impermeable marls, so the highest porosities are generally in the central parts of the aquifer.

5 WATER CHEMISTRY

5.1 Elements and Species in Water

Aqueous systems closed to the atmosphere and its surroundings contain a fixed total mass of components, but the amounts of present species vary together with other physical parameters by reactions and internal processes. That means that the material flow between the system and its surrounding must be zero (STUMM & MORGAN, 1996). Molal concentration (molality) of a dissolved substance in water is defined as:

$$m_i = \frac{n_i}{w_w} \quad (5\text{-}1)$$

where n_i is the number of moles of the i^{th} solute species and w_w is the mass in kilograms of solvent water**.**

Total concentrations of dissolved components can be obtained from the chemical analysis which leads to a mass balance equation:

$$m_{T,Ca^{2+}} = m_{Ca^{2+}} + m_{CaOH(aq)} + m_{CaCO_3(aq)} + m_{CaHCO_3^+} + \cdots \quad (5\text{-}2)$$

where $m_{T,}\,Ca^{2+}$is the total or analytical concentration (on molal scale, mol/kgw) and m_i is the molality of any individual chemical species contribution to the mass balance.

In complex solutions, ion concentrations are expressed as thermodynamic activity which is related to the molal concentration, m_i, by the relation:

$$a_i = m_i \gamma_i \quad (5\text{-}3)$$

where γ_i is the activity coefficient, a function of the composition of the aqueous solution (WOLERY& JAREK, 2003).

5.2 Solution Thermodynamics – Ionic Strength

Thermodynamics of solution approximates reality in terms of deviations from some defined ideal behaviour, so the parameters as activity coefficients are introduced.

The activity is an important physical parameter, but its value depends on the activity coefficients, γ. In ideal solutions activities are equal to concentrations, but in real solutions (e.g. highly concentrated salt solutions), activity coefficients are used for the correction of nonideality of the solution (STUMM & MORGAN, 1996). In diluted solutions, activity coefficients range from one (lower concentration) to zero (higher concentration). When a solution goes beyond ionic strength of 0.5M, activity coefficients do not continue to decrease with increase in ionic strength, but they start increasing and solvent changes (http://www.umich.edu/~chem241/lecture11final.pdf) (***Figure 5-1***).

As the activity coefficients are quite complex functions, it is difficult to obtain highly accurate results. Much of their behaviour depends on the ionic strength of the solution which is defined as:

$$I = \frac{1}{2}\sum_{i=1}^{n} c_i z_i^2 \quad (5\text{-}4)$$

where the summation is over c_i, molar concentrations (mol/l) of all aqueous solute species, and z_i is the electrical charge.

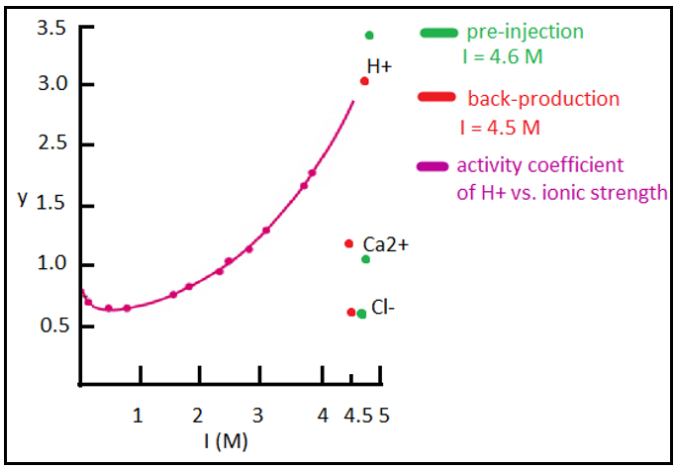

Figure 5-1 *Deviation of solution from the ideal; Ketzin´s brine.*

Activity coefficients go beyond one in the very saline solutions. On the graph is an example for three ions from the Ketzin´s brine. On the right-hand side, are shown activity coefficients of hydrogen, calcium and chlorine ions during the pre-injection test (green colour) and back-production test (red colour), where ionic strength was around 4.5 M. Curve describes activity coefficients of hydrogen ions in NaClO4 solution of varying ionic strengths (http://www.umich.edu/~chem241/lecture11final.pdf).

The usual range of ionic strength is from zero to eight, while for brines is around 5M. Salinity can also be expressed as the concentration of total dissolved solids (***Figure 5-2***).

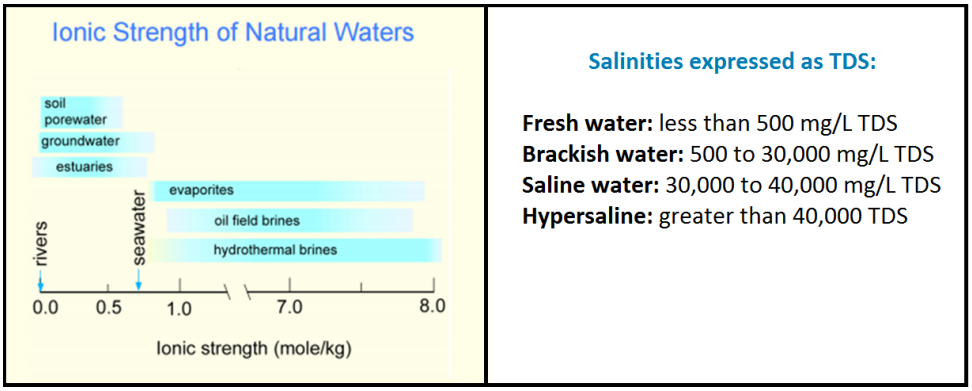

Figure 5-2 *Ionic strength of the different types of natural waters (left) and salinities expressed as total dissolved solids (TDS) for different types of natural waters (right).*

(http://mineral.gly.bris.ac.uk/AqueousGeochemistry/AqueousSolutionsI.pdf)

Model equations that are based only on ionic strength of the solution and exclude activity coefficients can be applied only to diluted solutions (WOLERY & JAREK, 2003).

5.3 Calculation of Activity Coefficients

A prerequisite for general accuracy is a thermodynamic consistency. According to WOLERY & JAREK (2003), the activity coefficient of each aqueous species depend on each other.

The Debye-Hückel equation is used for the calculation of activity coefficients in diluted solutions, very low ionic strengths. For more concentrated solutions, activity coefficient is determinated using Davies equation:

$$log\gamma_i = -Az_i^2\left(\frac{\sqrt{I}}{1+\sqrt{I}}\right) - 0.2I \quad (5\text{-}5)$$

where γ_i is the activity coefficients, I is ionic strength, A is a constant depending on temperature and dielectric constant of the solvent and z_i is the charge on the ion.

For the solutions that have ionic strength higher than 1M it is quite complicated to define activity coefficients, so the Pitzer equations are used instead. According to WOLERY & JAREK (2003), models based on these equations have been developed to describe solution properties together with the equilibrium between such solutions and salt minerals. Pitzer equations are based on a semi-theoretical interpretation of ionic interactions (PITZER, 1973), written in terms of interaction coefficients and parameters from which such coefficients are calculated.

5.4 Carbonate Equilibria

Natural waters obtain their equilibrium composition through a variety of chemical reactions and physicochemical processes. Thermodynamic, or equilibrium models for natural waters have been developed more extensively than kinetic models. They require less input parameters, but nevertheless a lot of things can be calculated with a proper accuracy. However, kinetic and equilibrium models are often needed in the same system (STUMM & MORGAN, 1996).

According to STUMM & MORGAN (1996), each case of this equilibrium can be represented by a mass-action equation for the dissociation of the ion-pair or complex. The calcium sulphate ion-pair dissociates according to the reaction:

$$CaSO_4(aq) = Ca^{2+} + SO_4^{2-} \quad (5\text{-}6)$$

$$K_{CaSO_4} = \frac{a_{Ca^{2+}} a_{SO_4^{2-}}}{a_{CaSO_{4(aq)}}} \quad (5\text{-}7)$$

where = is used as the sign for a reversible chemical reaction, K is the equilibrium constant and a_i represents the thermodynamic activity of each species.

Carbonate equilibrium in an aqueous system is defined with the set of equations given in the ***Table 5-1***.

Table 5-1 *Carbonate equilibrium (STUMM & MORGAN, 1996).*

$H_2O \leftrightarrow H^+ + OH^-$	$K_w = 10^{-14.0}$
$CO_2\ (g) + H_2O \leftrightarrow H_2CO_3$	$K_H = 10^{-1.5}$
$H_2CO_3 \leftrightarrow H^+ + HCO_3^-$	$K_1 = 10^{-6.3}$
$HCO_3^- \leftrightarrow H^+ + CO_3^{2-}$	$K_2 = 10^{-10.3}$
$CaCO_3(s) \leftrightarrow Ca^{2+} + CO_3^{2-}$	$K_{CaCO3}=10^{-8.35}$

Dissolution equilibrium is pH dependent when the species in the water undergo acid-base reactions (STUMM & MORGAN, 1996). Thus, carbonic acid dissociates in water as a function of pH (***Figure 5-3***).

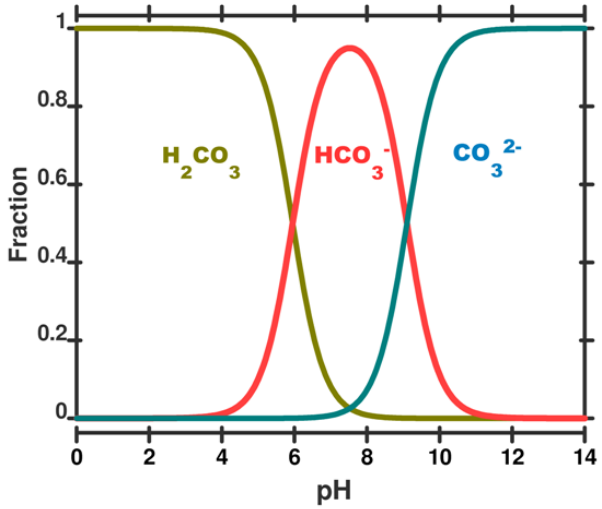

Figure 5-3 *A speciation diagram for the carbonic acid system in seawater as a function of pH (https://skepticalscience.com/print.php?n=888).*

As seen in ***Figure 5-3*** the y-axis gives the mole fraction of each species present. A vertical line drawn at any pH value gives the relative proportion of each species. This plot is simplified to illustrate the concept; in real seawater several other factors like salinity, temperature and pressure are important.

6 PHREEQC PROGRAM CALCULATIONS

6.1 Application to Reservoir Models

PHREEQC is a computer program for simulation of chemical reactions and transport processes that occur in natural waters, laboratory experiments, or in industrial processes. It is based on equilibrium chemistry of aqueous solutions that are interacting with minerals, gases and solid solutions.

The main objective of this study are stationary-state thermodynamic models which require the system to be closed, in this case, to the gas.

Boundaries of the observed natural systems, aquifers, are contacts with impermeable rocks at the bottom of the reservoir and contacts with the gas plume at the top. In the PHREEQC, the system boundary of the solution is free CO_2 gas above it. The heat and water flow were not implemented into this simulation. As the temperature and the concentration of elements here are vertically and horizontally relatively uniform, diffusion, convection and advection, are irrelevant.

One of the program capabilities is to obtain in situ physical parameters of aqueous solutions, brines, so the on-site and off-site measurements can be corrected. PHREEQC version 3.0. has been used for this study, and the input data edited in the Notepad ++. The initial step for acquiring this type of a model was an aquatic system observation followed by the laboratory experiments (***Figure 6-1***).

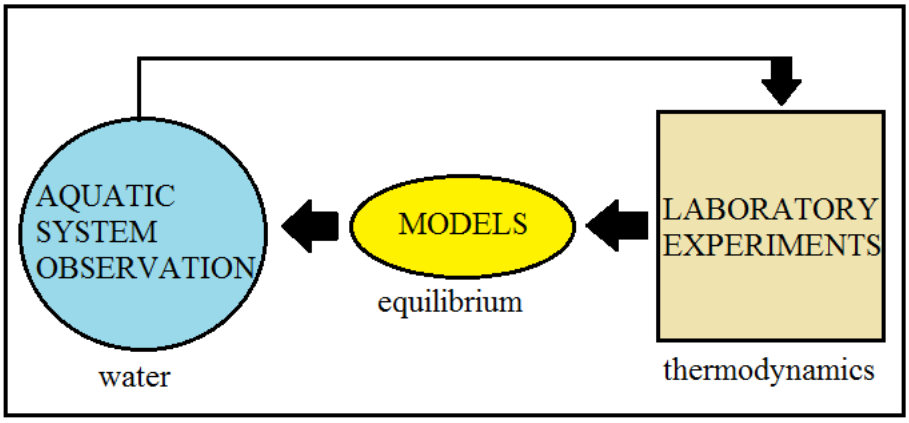

Figure 6-1 *Required steps for obtaining a model of an aqueous system.*

For the equilibrium model, the input data consist of solution composition with batch-reactions at the reservoir temperature and pressure. At first, program converts concentrations of elements (mg/l) into molal concentrations (mol/kg) which stay constant until the end of the simulation. The PHREEQC program assumes one kilogramme of water (1 kgw) and volume of approximately 1.1 litres if not set different. As mentioned previously, in these equilibrium models concentrations remain constant ***(Figure 6-2***), but saturation indices and physical parameters values change in each batch-reaction.

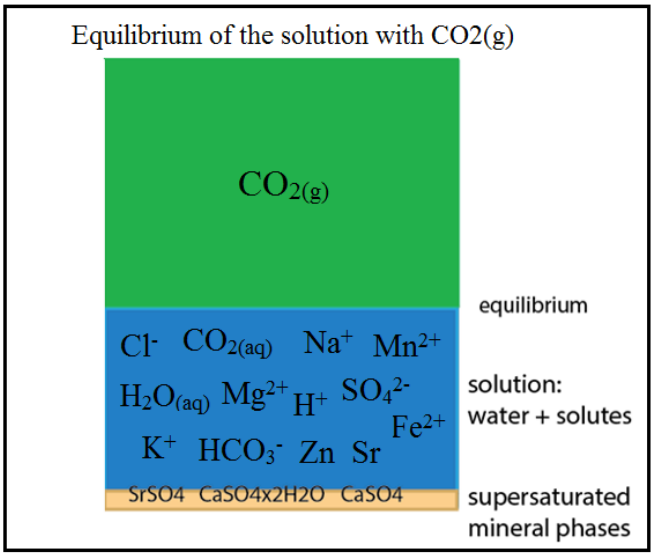

Figure 6-2 *Equilibrium model in the PHREEQC simulation. A free CO2(g) is a system boundary of the solution.*

Concerning trapping mechanisms, the focus of this study is on solubility and mineral trapping (***Figure 6-3***). CO_2 reacts with water and disrupts a natural equilibrium until the new one is established. Most models of solubility trapping assume instantaneous equilibrium between the brine and free $CO_{2(g)}$. The solubility of CO_2 varies as a function of pressure, temperature and salinity (SAYLOR & ZERAI, 2004). As trapping mechanisms prevent $CO_{2(g)}$ from migration to the surface, for long-term safety, it is crucial to correctly estimate which reactions will occur, their rates, how long it will take to attain new equilibrium, and how the system changes.

Figure 6-3 *Dense CO2(g) migrating upwards (light blue bubbles) dissolving and reacting with the grains of the rock, leading to precipitation of minerals on the grain boundaries (white) (CO2GeoNet, 2007) (http://online.fliphtml5.com/iomp/mtiw/#p=1)*

6.2 Calculation of saturation indices

The ionic strength of the solution, specific conductance, density, total alkalinity, total $CO_{2(g)}$ charge balance and electrical balance, activity coefficients of ions and species, activities, pH, pe, and some other less important parameters are carried out for each batch-reaction. Saturation indices are calculated with the following equation:

$$SI = \log IAP - \log K \quad (6\text{-}1)$$

where log IAP is a logarithm of ion activity product (actual activities in the water) and log K is a logarithm of equilibrium constant (activities in the state of equilibrium).

When a saturation index is zero, a mineral phase is in equilibrium with the solution, below zero is undersaturated, and above zero supersaturated. However, crystals mostly occur when saturation index is above one. Based on the regimes of crystal growth for ionic substances, supersaturated minerals are firstly metastable, then undergo heterogeneous nucleation, and at high saturation homogeneous nucleation (APPELO & POSTMA, 1996). The program calculates all the mentioned parameters simultaneously, and in that way it is possible to observe the influence of each input parameter on the solution behaviour. However, accuracy and extent of the results depend on the consistency and scope of the input data and used database. Database for ionic strengths over 1M (Pitzer) is very scarce and it does not contain data for alumosilicates which is necessary if the rock-forming minerals are included.

Any information from petrographic analyses of the reservoir core samples can be helpful for adjusting target saturation indices of mineral phases: which crystals have been found to attain equilibrium with them; the keyword equilibrium phase is used for reversible reactions of the solution with given mineral phases, and the keyword reaction for irreversible reactions in the solution.

7 PHREEQC MODELS OF THE REGIONAL DSA POLJANA AND THE KETZIN STORAGE SITE

7.1 Deep Saline Aquifer Poljana

7.1.1 Statistical Analysis of Porosity Distribution

The porosities obtained from 18 wells with a few well-logging methods by INA d.d were used as the input data together with the mean depth and effective thicknesses of the Deep Saline Aquifer Poljana (DSA Poljana) for obtaining a 3D scatter (***Figure 7-1***) and 2D contour plot (***Figure 7-2***). The highest porosity is at the location of the lowest depth and the greatest thickness of the aquifer (well BS-1). The regression plane predicts that porosity decreases with depth and where the thickness is lowest (well Vel-1) (***Figure 7-1***).

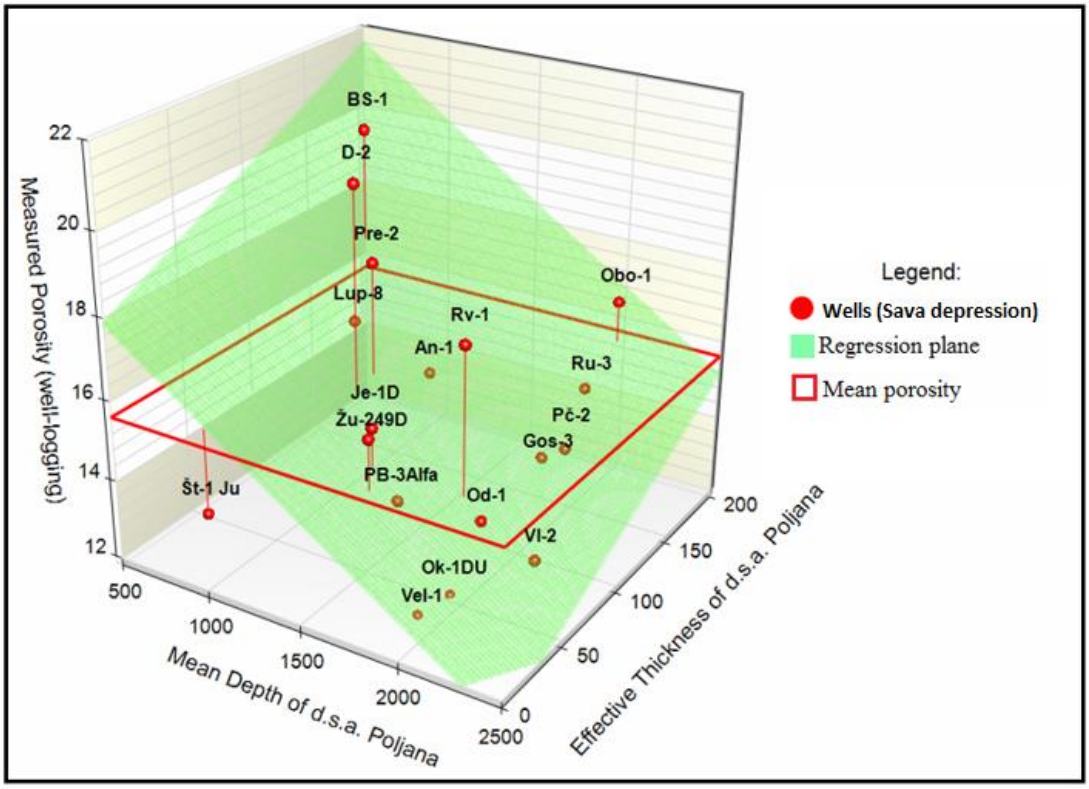

Figure 7-1 *3D scatter plot of measured porosity vs effective thickness. Green coloured is a regression plane (location of deep wells taken from KOLENKOVIĆ, 2012).*

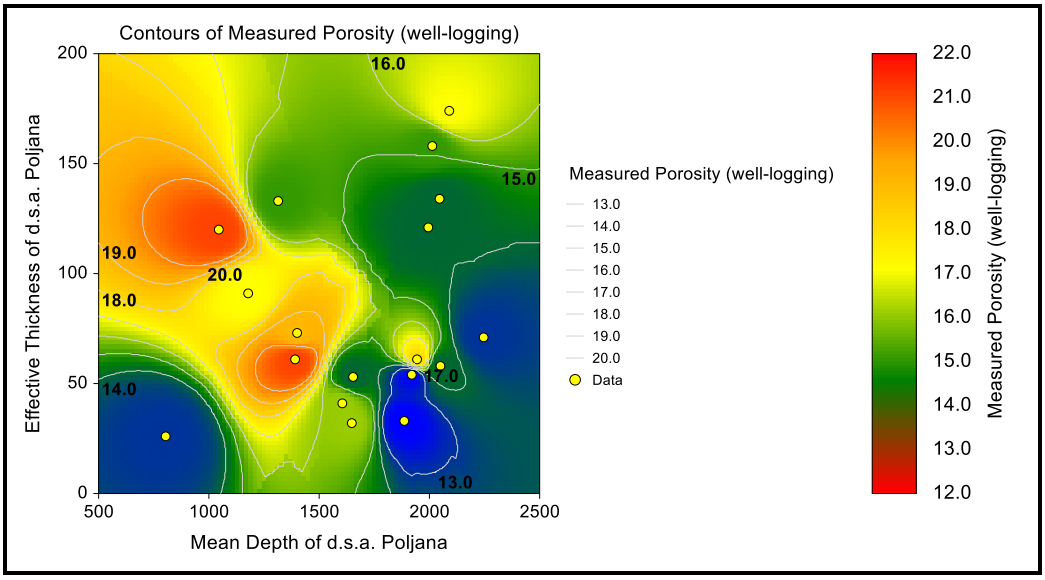

Figure 7-2 *Contour plot of measured porosity values vs. mean depth and effective thickness of DSA Poljana (SAFTIĆ et al., 2015).*

Such a porosity model is only valid for the wells with the depth and thickness values lying in the input data range. There is a mildly negative correlation between the porosity and depth and a more pronounced positive one between the porosity and thickness of sandstone layers (SAFTIĆ et al., 2015).

7.1.2 Multiple Regression

Multiple regression analysis with two independent variables (mean depth and effective thickness) has been used for the extrapolation of the porosity values estimated (obtained by interpretation of well logs) at 18 wells (measured porosity) to 60 other wells for which the mean depth and effective thickness of the Poljana aquifer were known ***(Appendix 1)***. The analysis has been done in the NCSS statistical software. It resulted in similar values as the analysis done in Microsoft Excel program by RISEK (2013). Porosity values are calculated with the equation:

$$\phi = 19.4864 + 0.0186 * \text{Effective Thickness} - 0.0032 * \text{Mean Depth} \quad (7\text{-}1)$$

Coefficient of determination, R^2 for the effective thickness is 0.03989 and for the mean depth 0.2576. This indicates better correlation between porosity and mean depth than between porosity and effective thickness.

From the residual plots it is clear that this approach, in general, is not very precise as the values are quite scattered, but it still gives some approximations (***Figure 7-3***). Residuals are calculated with the equation:

$$e = y - \hat{y} \quad (7\text{-}2)$$

where e is a residual, y is an observed value and ŷ is a predicted value.

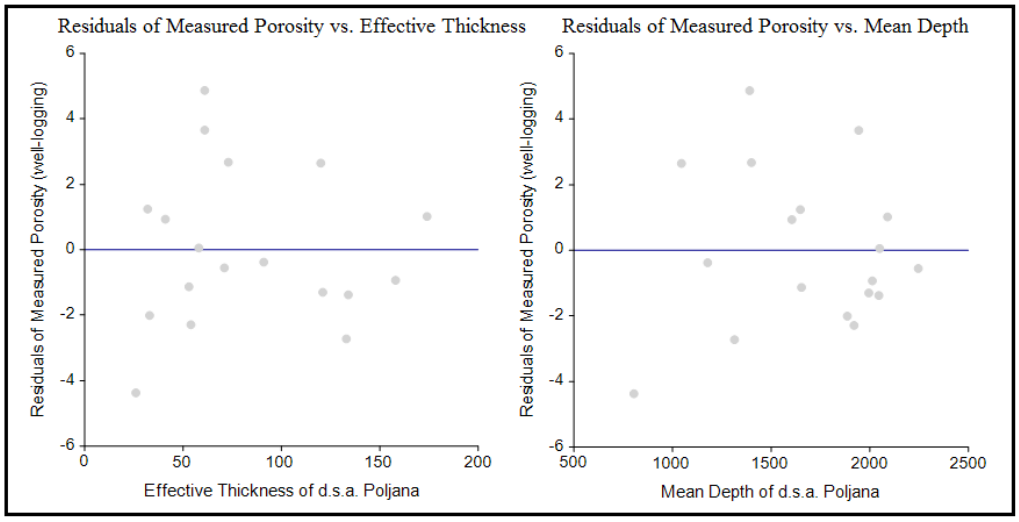

Figure 7-3 *Residuals of measured porosity.*

In the histogram, percentages of the total frequency of residuals of measured porosities are pointed out. Most of the values have been just slightly changed, but still, some of them have been changed considerably (***Figure 7-4***).

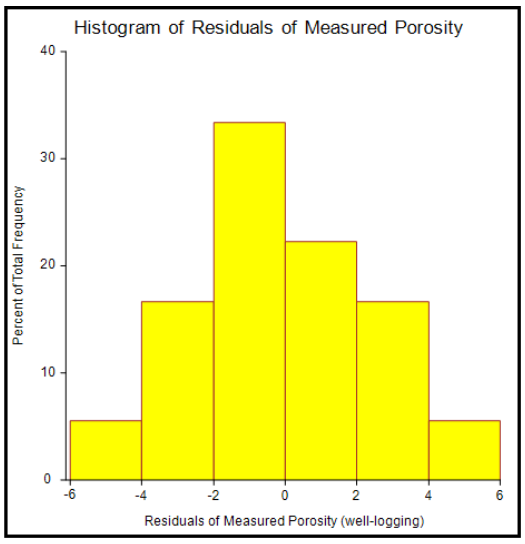

Figure 7-4 *Histogram of residuals of measured porosity.*

7.1.3 Input Data – the Žutica well

The only available data from water analysis in the Western part of Sava depression was from the deep well Žu-249D. One complete analysis of water chemistry was done in January 2014, and the another in October 2014 by INA d.d. (***Appendix 2***). Water composition is more or less similar and both of them have traces of oil and chemicals. The actual depth of the analysed water is unknown at this moment, but based on the salinity and the lithostratigraphic column (Figure 3-5), it is most probably from the Poljana sandstones. Data are not reliable, it can also be that at least a part of this water migrated from the deeper aquifer. However, the salinity of the DSA Poljana formation water is not thoroughly explored, but some of the previous analyses gave extremely low values. There is only one reliable result from the Oborovo-1 well nearby, where the salinity is 18230 mg/l NaCl (KOLENKOVIĆ, 2012). According to the electro-log diagram interpretations from the discussed area, the salinity of the Poljana aquifer is in the range of 18000 to 58000 mg/l NaCl (KOLENKOVIĆ, 2012), and this water´s salinity is around 33000 mg/l NaCl. From of the two available water analysis, the one from October 2014 has been used for modelling because of the lower percent error in charge balance calculated manually and in the PHREEQC program (***Appendix 3***).The solution must be electrically neutral, should have a specific ratio of cations and anions that maintain a net balance between positive and negative charge:

$$Electro\ Neutrality\ (\%) = \frac{(Sum\ cations + Sum\ anions)}{(Sum\ cations - Sum\ anions)}\ x\ 100 \quad (7\text{-}3)$$

The two models have been made in the following way. One with the Pitzer database, and the other with the PHREEQC database which is only adequate for lower salinities (low ionic strengths) as it may break down at higher ionic strengths (in the range of seawater and above). It consists of fewer mineral phases, but it calculates pe from the present redox couples (http://wwwbrr.cr.usgs.gov/projects/GWC_coupled/phreeqc/html/final-4.html).

A list of input parameters, which had been estimated for the Poljana sandstones at the location of Žu-249D well (KOLENKOVIĆ, 2012), is shown in the ***Table 7-1***.

Table 7-1 *Certain parameters at the mean depth of the DSA Poljana in the location of well Žu-249D taken from KOLENKOVIĆ (2012).*

Well Žu-249D – Poljana Sandstones	
Mean depth	1648 m
Temperature	83°C
Porosity	16%
Temperature gradient in the western part of Sava Depression	4.36°C/100 m
Hydrostatic pressure	165 bar
CO_2 density	470 kg/m^3
Effective thickness of sandstone layer	32 m
Relative depth of cap rock (marl)	1610 m

7.1.4 Results – the Žutica well

First batch-reaction has been at the reservoir temperature of 83°C and pressure of around 1 bar, and the second one with the partial pressure of $CO_{2(g)}$ of 165 bar at the reservoir temperature of 83°C. The temperature of the initial solution was 25°C, and pH 6.8 (***Appendix 4)***. Saturation indices are temperature dependent so their values have changed after both batch-reactions. The reasons for that change are, in fact, ion activity products and equilibrium constants. Specific conductance increased, and the pH decreased (***Table 7-2***). Activity, activity coefficients, and molalities of the all polyatomic species have also changed.

***Table 7-2** Žutica – parameters.*

Žutica-249 **Date:** **15.10.2014**	**Temperature [°C]**			
	25	83	83	
	$pCO_{2(g)}$ [atm]			
	≈1	≈ 1	162.8 ------fugacity----- 97.35 atm	
	Reaction pressure [atm]			
	/	162.8	162.8	
Database	***pitzer.dat***			***phreeqc.dat***
pH	6.8	6.682	4.142	4.129
Spec. Conductance [µS/cm³]	58521	150243	162092	135895
Ionic strength	0.657	0.657	0.657	0.655
Total CO_2 = total C [mol/kgw]	0.0146	0.0146	1.262	1.205
HCO_3^- [mol/kgw]	0.01207	0.01204	0.0122	0.0132
H_2CO_3 [mol/kgw]	0.002508	0.002522	1.250	1.014
pe	/	/	/	7.120

The final result of modelling, saturation indices, are shown in the ***Figure 7-5*** and ***Figure 7-6.*** After the addition of $CO_{2(g)}$ into the simulation, all carbonates and sulphates became undersaturated as pH decreased and the H_2CO_3/HCO_3^- ratio increased (***Table 7-2***).

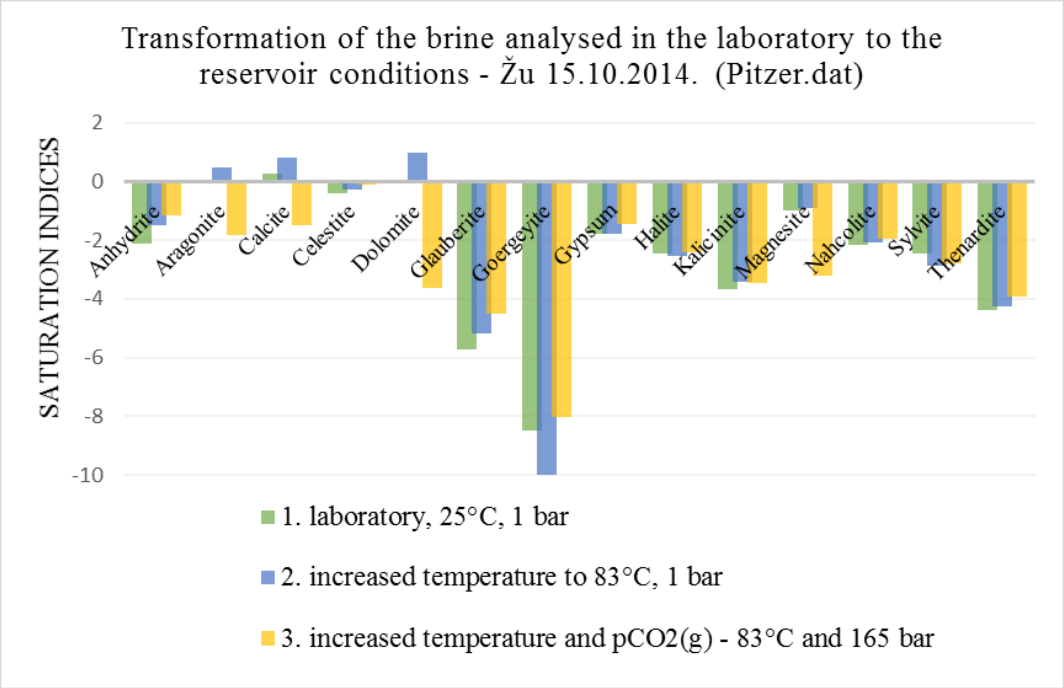

Figure 7-5 *Transformation of the brine analysed in the laboratory to the reservoir conditions – Žutica well, 15.10.2014.*

The same trend was observed after using both databases, Pitzer and PHREEQC. However, because of the presence of redox couples in the PHREEQC database, goethite and hematite are present in the output and they became supersaturated after the addition of $CO_{2(g)}$ (***Figure 7-6***).

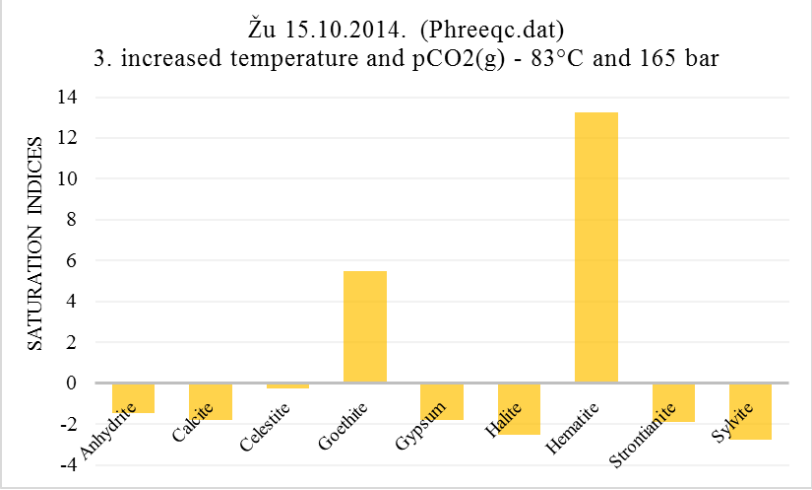

Figure 7-6 *Third step of the simulation with the PHREEQC database.*

Concerning previously mentioned trapping mechanism this is equal to solubility trapping. From this type of simulation is only possible to see which minerals could precipitate

in the certain solution at the given pressures and temperatures, but it is not likely that all of them would precipitate in natural systems. Moreover, the output highly depends on the minerals in the database which is visible from these two results (***Figure 7-5***) (***Figure 7-6***).

7.2 Ketzin

7.2.1 Back-production Test

The reservoir back-production test was carried out from October 16, 2014 to October 27, 2014. Fifty-four cubic meters of water were pumped out from the reservoir ***(Figure 7-7)***.

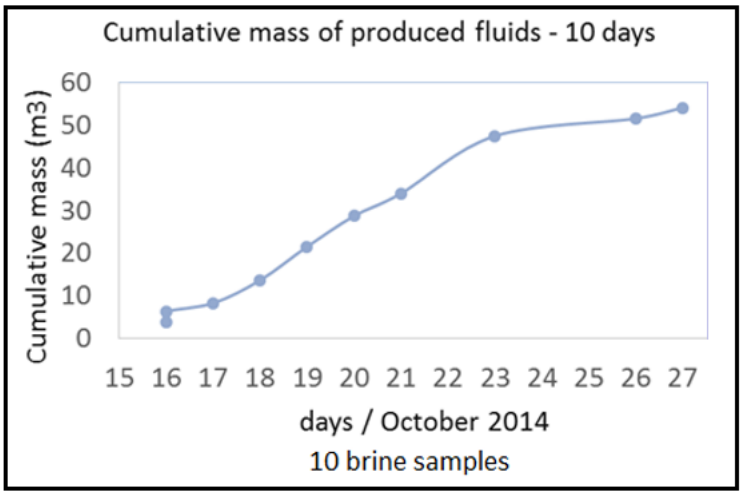

Figure 7-7 *Cumulative mass of produced fluids during the back-production test (data from water analyses of PWU and GFZ).*

The $CO_{2(g)}$ was released into the atmosphere and the brine disposed of. The aim of the test was to gather data about the pressure and temperature evolvement during releasement of CO_2, and about the chemical composition of produced brine and CO_2 (MÖLLER et al., 2015).

During the test, Potsdamer Wasser-und Umweltlabor (PWU) and German Research Centre for Geosciences (GFZ) were doing chemical analyses of water. Temperature, pH and conductivity were measured on the site, soon after the water had been pumped out. It is important to measure those parameters not later than few hours after the water reaches a surface because carbon dioxide degassing increases pH, water absorbs or releases heat, and conductivity is a measure of temperature and concentration of ions.

In the laboratory pH, temperature and conductivity measurements were repeated together with analyses of oxygen content and redox voltage. As expected, the oxygen content was very low, which is linked to impurities, and redox voltage corresponds to a reducing environment. The concentration of anions and cations, hydrogen carbonate content, dissolved organic carbon and water density have also been measured there. GFZ additionally analysed cations and metals (Sr^{2+}, Zn^{2+}) as the concentrations of cations obtained by PWU were incorrect according to the charge balance error.

In-situ reservoir, temperature and pressure were obtained from the bottomhole measurements. The temperature was 34°C and partial pressure of $CO_{2(g)}$ corresponded to 64.64 bar. Bottomhole pressure had dropped to approximately 59 bar at the beginning of the back-production test (***Figure 7-8***), but when the test had finished, it reached the previous value (WIESE B., 2014).

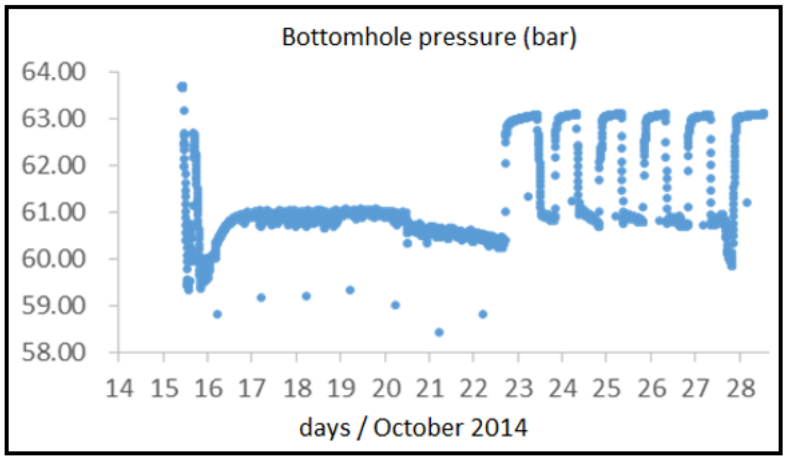

Figure 7-8 *Variation of bottomhole pressure during the back-production test (WIESE B., 2014).*

7.2.2 Input Data – Ketzin

Three models have been made for this study using three different sets of input data:

1) Water composition six years after the injection (back-production test);

a) First day of back-production test (***Appendix 5***);

b) Last day of back-production test (***Appendix 6***);

2) Water composition prior the injection (baseline composition) (***Appendix 7***).

The initial solution consists of analysed concentrations of anions by PWU and cations by GFZ, laboratory water temperature of 19°C, pH of 6.0 and total inorganic carbon of 2423.1 mg/l. All three simulations were run using Pitzer database.

Only iron concentration has linear dependence over the cumulative mass of produced fluid. The cause is probably corrosion on the walls of the wellbores which has been cleared out during the water pumping, so the iron concentration has constantly been dropping until the last three days. Sodium and other ions do not show any linear dependence over the cumulative mass of produced fluid (***Figure 7-9***). As only iron concentration changes remarkably any of the water analyses could be used for this simulation. There is no difference in using water composition from the first day or the last day, but anyway, the best option is always an average value from the all water samples.

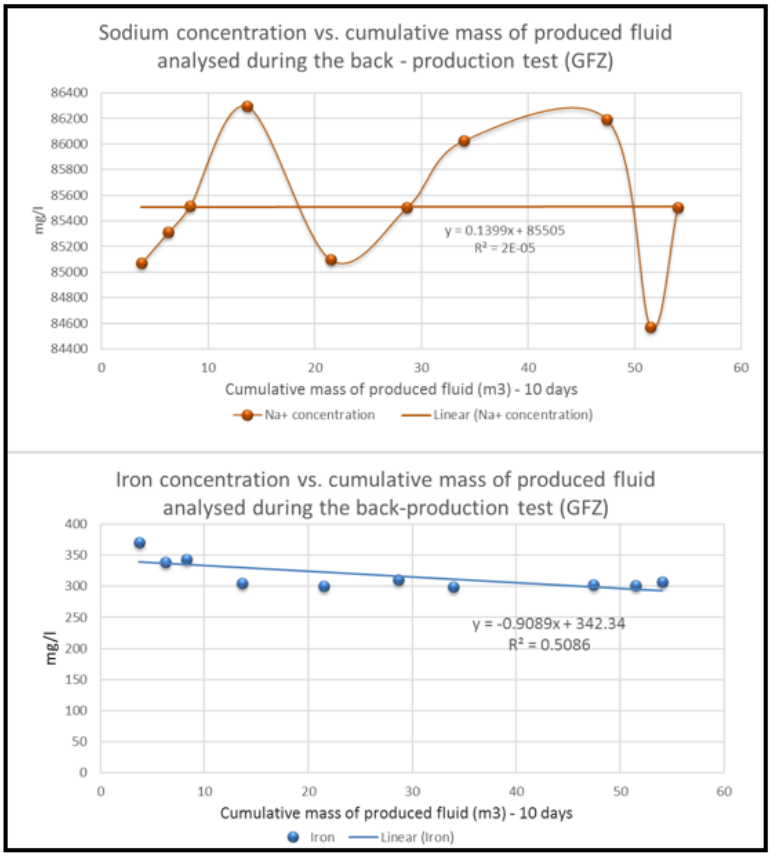

Figure 7-9 *Sodium and iron concentration over cumulative mass of produced fluids (Data taken from the water analyses of GFZ and PWU).*

For non-ideal solutions, pressure and concentration are expressed in terms of fugacity and activity (STUMM & MORGAN, 1996). The ideal gas pressure and fugacity are related through the dimensionless fugacity coefficient, φ:

$$\varphi = f / P \quad (7\text{-}4)$$

where f is fugacity and P is a partial pressure. For an ideal gas, fugacity and pressure are equal so φ is 1.

7.2.3 Results – Ketzin

7.2.3.1 First Day of Back-production Test

First batch-reaction has been at the reservoir temperature of 34°C, pressure was approximately 1.5 bar, and the second one with the partial pressure of $CO_{2(g)}$ of 64,64 bar at the reservoir temperature of 34°C (***Appendix 5***).

1) First batch-reaction

As result of first batch-reaction specific conductance increased and pH decreased (***Table 7-4***). Activity coefficients, molalities and activities have changed. The amount of total dissolved gas stayed the same. Henry`s law is used for the calculation of solubility of ideal gases, a quotient of concentration and pressure (PARKURST et al., 2012). Thus, it stayed constant as the amount of carbon and pressure did not change.

Carbonates and sulphates which do not have water molecules in their structure are more saturated at a higher temperature. In this model, dolomite is the most supersaturated mineral phase, and that can be correlated with the solubility constants from thermodynamic data. The negative logarithm of the equilibrium constant (-logK) of dolomite is 17.09, calcite 8.48 and aragonite 8.35. Salts (chlorides and some sulphates) are more soluble at a higher temperature. Anhydrite is more saturated than gypsum ($CaSO_4$ x $2H_2O$), and aragonite is less saturated than calcite (***Figure 7-10***). Cement phase-portlandite ($Na_2Ca(SO_4)_2$) is more stable at a higher temperature.

2) Second batch-reaction

Conductivity has been just slightly changed and pH decreased (***Table 7-4***). Conductivity strongly depends on the temperature. The density of the solution decreased, and volume increased. Approximately 66 kg/cm^2 of $CO_{2(g)}$ has been added to the system throughout reversible reactions with the initial solution at 34°C. The total amount of dissolved CO_2 increased because of $CO_{2(g)}$ addition to the system. The solubility of gases in this case is

calculated with the Peng-Robinson equation which is valid for the non-ideal gases or real gases (PARKHURST et al., 2012). Here, the pressure is expressed as a fugacity and the concentrations in the form of activities.

All carbonates are undersaturated, while all sulphates are more saturated or supersaturated in comparison with the first batch-reaction and saturation indices of salts have been slightly changed towards positive saturation. Here, gypsum ($CaSO_4x\ 2H_2O$) is more saturated than anhydrite ($CaSO_4$), and aragonite ($CaCO_3$) less saturated than calcite ($CaCO_3$), the same as before. The amount of HCO_3^- species have slightly increased so kalicinite ($KHCO_3$) and nahcolite ($NaHCO_3$) became more saturated (***Figure 7-10***).

Table 7-3 *Physical parameters – back-production test – October 16, 2014.*

Back-production test Date: 16.10.14. 11:15 pitzer.dat	**Temperature [°C]**		
	19	**34**	**34**
	$pCO_{2(g)}$ [atm]		
	≈1	≈ 1.5	64 ------*fugacity*----- 44.67 atm
	Reaction pressure [atm]		
	/	64.64	64.64
pH	6	5.901	4.463
Spec. Conductance [µS/cm³]	272068	388960	389259
Ionic strength	4.45	4.45	4.45
Total CO_2 [mol/kgw] = Total C	0.06428	0.06428	0.6174
HCO_3^- [mol/kgw]	0.04336	0.04336	0.04354
$H2CO_3$ [mol/kgw]	0.02084	0.02084	0.5739

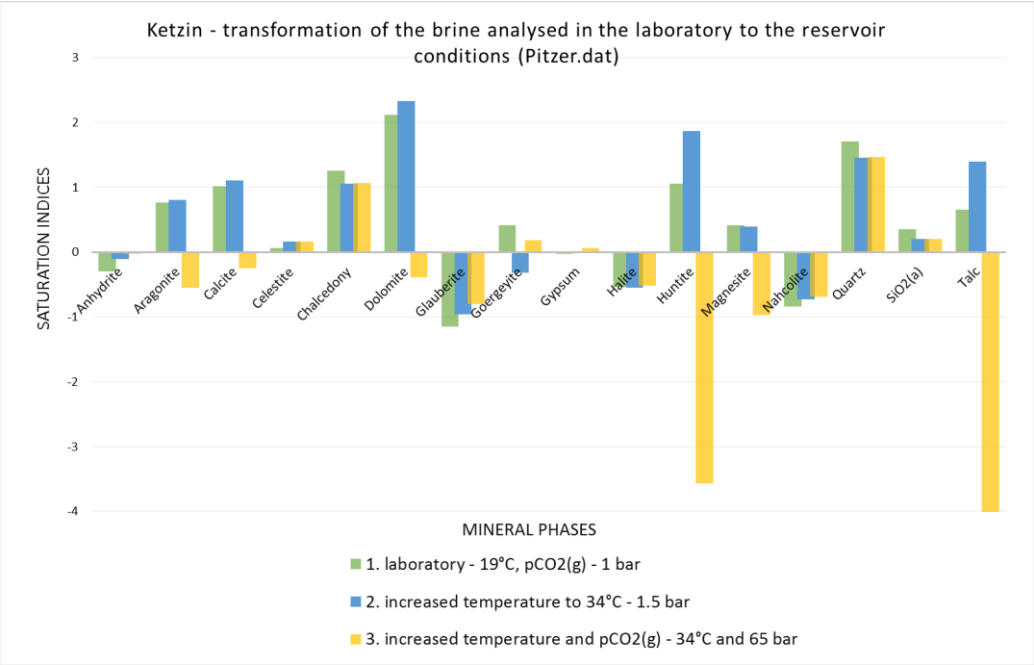

Figure 7-10 *Saturation indices of mineral phases for three steps of batch-reactions.*

7.2.3.2 Comparison of Water Analysed Prior the Injection, on the First and the Last Day of Back-production Test

During the pre-injection test, 78.7 m^3 of water has been pumped out from the well Ktzi-202. A complete water analysis has been done in the laboratory. Prior to the injection and during the back-production test, the main physical parameters and ions have been measured, in order to compare the new composition with the baseline survey**.** The average values of concentration of ions from days when the waters have been analysed were used for their comparison (***Figure 7-11***).

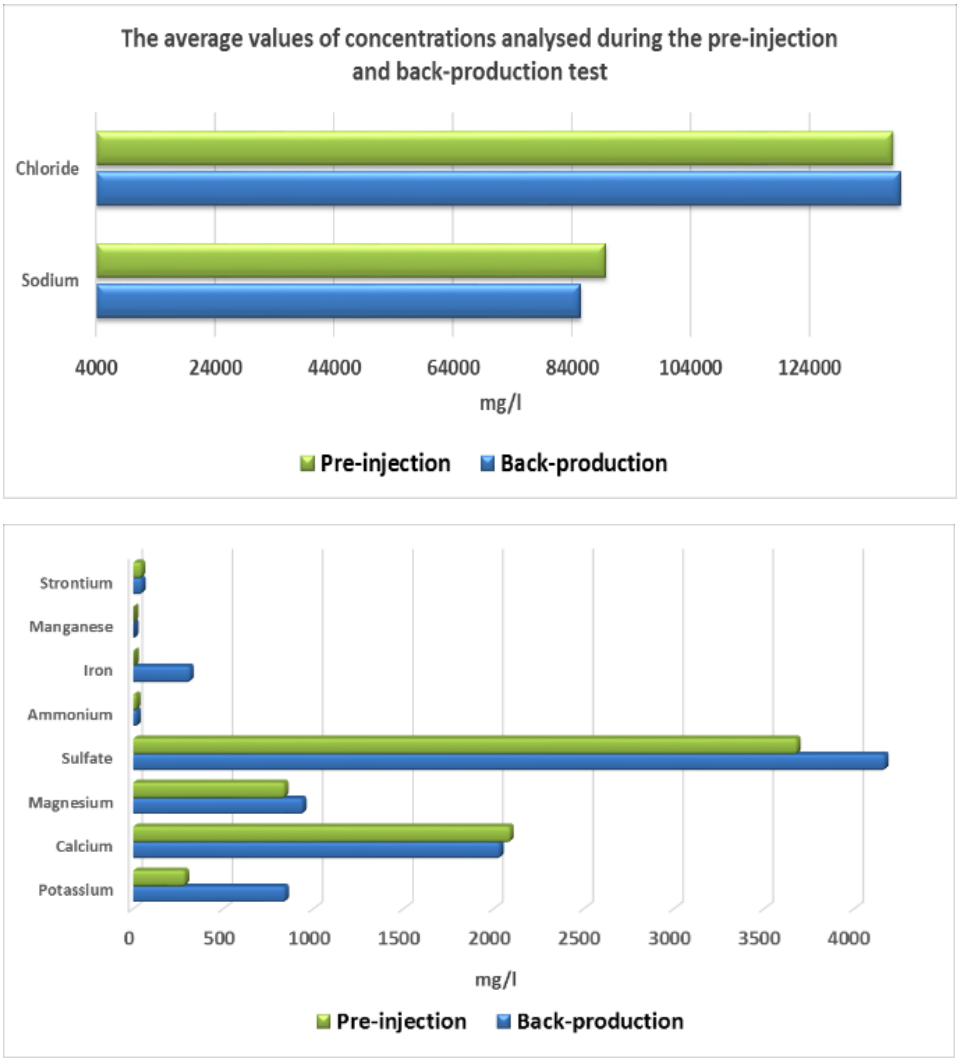

Figure 7-11 *The average values of concentration of ions in mg/l that have been analysed during the pre-injection and back-production test.*

Chloride and sodium kept a constant ratio, which is normal in groundwaters. Salinity in Ketzin is very high, approximately 226400 mg/l TDS. Chloride concentration did not change at all, as it is the most conservative element. Small variations can be due to analytical errors. Sodium is also a conservative element, but it could be removed from the solution by precipitation of some alumosilicates, e.g. analcime ($NaAlSi_2O_6x(H_2O)$) which has been found as a precipitate in some other CO_2 projects unrelated directly to Ketzin. Sodium and calcium concentration have slightly decreased after the injection. Precipitation of gypsum could have an impact on the lower amount of calcium. The higher amount of potassium can be from the dissolution of K-feldspars and illite which are two of the reservoir rock-forming minerals and no precipitation of potassium salts has been found that could incorporate potassium from the brine.

Iron, sulphate, magnesium and potassium concentrations have increased after the injection. Additional iron could be from the dissolution of hematite (Fe_2O_3) or connected with the corrosion of wellbores, higher amount of sulphate from the dissolution of anhydrite, which is the most abundant reservoir cement phase, and magnesium from the dissolution of dolomite. Strontium, manganese, and ammonium are minor constituents and their concentration did not change (***Figure 7-11***).

There is not a significant difference between the water from first and the last day of back-production test, neither in the concentration (input data) nor in the output of the PHREEQC modelling (***Table 7-5***).

Table 7-4 *Physical parameters.*

pitzer.dat Final results of the modelling	**PRE-INJECTION TEST**	**BACK-PRODUCTION**	**BACK-PRODUCTION**
	average values from three water analyses	**16.10.14 11:15**	**27.10.14 10:30**
Reservoir pressure	**pCO_2(g) [atm]**		
64.64 atm	**0.012**	**64.64**	**64.64**
pH	6.387	4.463	4.41
Specific Conductance [µS/cm^3]	405361	389275	389559
Ionic strength	4.597	4.45	4.447
Total CO_2 [mol/kgw] = Total carbon (mg/l)	0.00116	0.617	0.612
HCO^{3-} [mol/kgw]	0.00101	0.0435	0.0384
H_2CO_3 [mol/kgw]	0.000146	0.574	0.574

Prior to the injection, pH of the brine was higher. Conductance and ionic strength was higher too and the reason for that is slightly higher salinity prior the injection (higher concentration of sodium and chloride ions) which can be due to analytical errors (***Table 7-5***).

Prior to the injection, calcite ($CaCO_3$), celestite ($SrSO_4$), dolomite ($CaMg(CO_3)_2$) and quartz (SiO_2) were supersaturated. After the injection of $CO_{2(g)}$ carbonates became undersaturated, while sulphates (gypsum, celestite, georgeyite ($Na_2Ca(SO_4)_2$) became

supersaturated. Chalcedony (SiO_2) and $SiO_{2(a)}$ remained supersaturated. Also, nahcolite ($NaHCO_3$) became more saturated due to the higher amount of HCO_3^- (***Figure 7-12***).

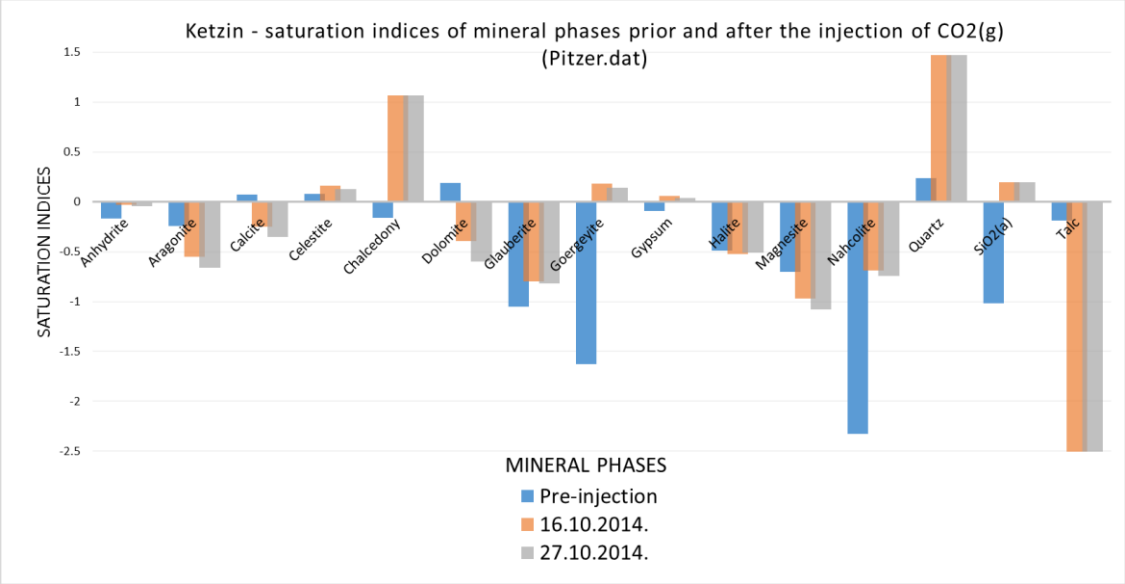

Figure 7-12 *Saturation indices.*

8 DISCUSSION

DSA Poljana potential storage unit and Ketzin pilot storage site have quite a similar mineral composition of reservoir rocks. The most abundant rock-forming minerals are quartz, feldspars, illite, mica, and dolomite as a cement phase. In Ketzin, hematite and pyrite are present as iron minerals, and the Upper Miocene sandstone reservoirs in the Sava depression contain iron in a form of Fe-rich carbonate cement phase, so it might be present in the Poljana sandstones, too. Both are fine grained channelized sandstone bodies but formed in different depositional paleo-environments.

Porosity in Ketzin ranges from 5 to 35%, and in DSA Poljana from 12 to 21%. Cap-rocks are pelitic sediments of low permeability. In the Western Sava Depression, targeted sandstone reservoirs are much deeper, so temperatures and pressures are quite higher, but salinity is much lower and, in that way, more suitable for modelling in the PHREEQC program. More or less, the same ions have been determined in waters from both storage sites and it turned out that both have a similar ratio of those ions, with a difference that in Ketzin concentrations are quite higher.

For the pre-injection test water has been pumped out from the other well and that might be the reason for slightly higher ionic strength and conductivity carried out in the simulation. The other reasons might be the differences in analytical equipment and errors in measurements.

During the 10 days of back-production test in Ketzin, the models show same results: a decrease in pH, dissolution of carbonates and precipitation of sulphates - gypsum ($CaSO_4$), celestite ($SrSO_4$) and georgeyite ($K_2Ca_5(SO_4)x6H_2O$) (***Figure 8-1***).

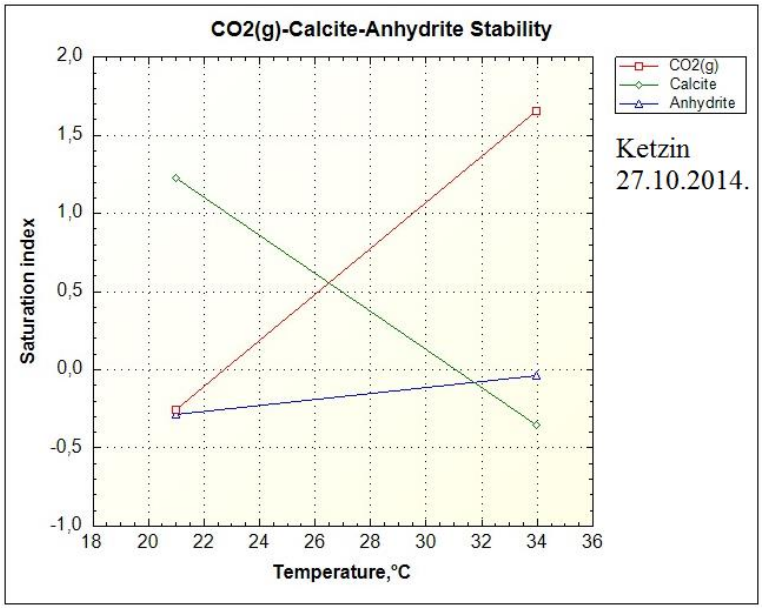

Figure 8-1 *Plot of CO2(g) – Calcite-anhydrite stability at different temperature (Ketzin back-production 16.10.2014; pitzer.dat).*

Modelling of the Žutica site in DSA Poljana resulted in quite a similar trend, dissolution of carbonates and a rise in saturation indices of sulphates, but both remained undersaturated. Moreover, there are some obscurities about sulphates in modelling extremely saline waters, like the one from Ketzin, for which none of the available databases is completely accurate.

Concerning the statistical analysis in the NCSS software, the sandstone reservoir at the location of the Žu-249 well is of moderate quality for a potential storage unit because the sandstone reservoirs drilled in some of the other wells are shallower, have a higher porosity, greater thickness, and higher estimated storage capacity. Anyway, as there are no other data from water analyses, this one, at least, gives us some insights into what might happen in reservoirs of similar water composition, temperature, and pressure.

This PHREEQC simulation (thermodynamical models) is an inexpensive way to monitor changes in reservoir rocks and water. It is useful to accompany each water analysis with this type of modelling. Pressure can be adjusted so that is a good way to approximate what might happen in a case of pressure changes over a certain period of time. Because of much lower salinity, water from Žutica well has been modelled using both Pitzer and PHREEQC database. PHREEQC database contains redox couples, so pe has been calculated, but its accuracy of modelling of extremely saline waters like Ketzin´s is questionable.

Thermodynamic, or equilibrium models can be done with only a few input parameters, but they are nevertheless powerful when applied within their proper limits. Kinetic reactions require more data (the initial mass of each rock forming mineral, reactive surfaces, equilibrium constants, formation enthalpies, and so forth), with a coexisting experimental work (PARKHURST & APPELO, 2012), and that should be the next step.

9 CONCLUSION

The most important findings from these simulations are that the injection of $CO_{2(g)}$ lowers pH of water and under the new circumstances certain mineral phases precipitate while some dissolve. In this way, $CO_{2(g)}$ is very slowly being removed from the brine.

As hydrations is a very fast process, the injected $CO_{2(g)}$ dissolves instantly and a new equilibrium state is established. Dissolution of rocks and incorporation of $CO_{2(g)}$ in the new mineral phases is a slow process. Comparing water samples from the pre-injection and the back-production it is clear that the water composition has not changed a lot after the injection, over 6 years, a period of experiment duration.

Conductivity was higher prior the injection and it could be connected with the $CO_{2(g)}$ injection as some of the ions have been removed from the brine by precipitation of secondary mineral phases under the new conditions.

Oil traces have been found in the water samples from Žutica field and its salinity is quite lower than in the Ketzin. As the salinity of Ketzin´s brine is extremely high, it was possible to have a $CO_{2(g)}$ storage unit in such a shallow aquifer. Temperature and pressure are quite low, but sufficient for $CO_{2(g)}$ to reach a supercritical state.

The both reservoirs are in deep saline aquifers, but much different concerning depth, salinity, burial history, so it is impossible to have an overall conclusion about chemical reactions in deep saline aquifers, although the mineral composition is quite similar.

Anyway, the same approach can be used in surveys of aquifers of up to moderate salinity. As there is no an adequate database for extremely saline brines, the results of Žutica´s water are more precise.

Both Ketzin and Žutica models are showing a decrease in pH and dissolution of carbonates, but in Ketzin´s model sulphates have been supersaturated, and in model Žutica understaturated, but less undersaturated than before the addition of CO_2. The reason is probably lower concentration of calcium and sulphate in Žutica´s water, and an overall lower concentration of ions. One important thing found in this study is that sulphates tend to precipitate under these circumstances triggered by the injection of $CO_{2(g)}$.

As it has been already known, $CO_{2(g)}$ is less soluble in more saline waters, under higher temperature and lower partial pressure which is just confirmed with this simulation.

The second step of this work would be kinetic modelling, but it requires more experimental data. From the themodynamic models is impossible to see how fast reaction are, but at least we know that water composition has not changed much in six years.

In a case of Ketzin is important to extend Pitzer database whether with the interpolation or experimental work to get more accurate results.

As these types of aquifers are closed naturals systems, $pCO_{2(g)}$ is not constant and it is expected to be slowly decreasing over time.

10 REFERENCES

10.1 Published

ANGUS, S., B. ARMSTRONG AND K.M. DE REUCK(1973): International Thermodynamic Tables of the Fluid State Volume 3. Carbon Dioxide. IUPAC Division of Physical Chemistry, Pergamon Press, London,vpp. 266–359.

APPELO, C. A. J., & POSTMA, D. (1996): Geochemistry, groundwater and pollution. Rotterdam, A.A. Balkema, 4th edition,522p.

DOUGHTY, C., PRUESS, K., BENSON, S.M., HOVORKA, S.D., KNOX, P.R. & GREEN, C.T. (2001): Capacity Investigation of Brine-Bearing Sands of the Frio Formation for Geologic Sequestration of CO_2. Proceedings of First National Conference on Carbon Sequestration, U.S. Department of Energy, National Energy Technology Laboratory.

EU GEOCAPACITY (2009): Assessing European Capacity for Geological Storage of Carbon Dioxide, Final Report, Geological Survey of Denmark and Greenland.

FISCHER, S. (2013), Mineralogical-geochemical effects during geological storage of CO_2 – Experimental investigations and geochemical modelling. Scientific Technical Report 13/13, GFZ German Research Centre for Geosciences.

FISCHER S, LIEBSCHER A, ZEMKE K, DE LUCIA M, Ketzin Team (2013): Does Injected CO_2 Affect (Chemical) Reservoir System Integrity? -A Comprehensive Experimental Approach. Energy Procedia; 37: 4473-4482, doi:10.1016/j.egypro.2013.06.352.

FÖRSER, A., SCHÖNER, R., FÖRSTER, H.-J., NORDEN, B., BLASCHKE, A.-W., LUCKERT, J., BEUTLER, G, GAUPP, R., and RHEDE, D.(2010): The Upper Triassic Stuttgart Formation (Middle Keuper) at Ketzin: The reservoir for pilot CO_2 storage in the Northeast German Basin. Mar. Pet. Geo., in press.

IPCC (2005): IPCC Special Report on Carbon Dioxide Capture and Storage. Prepared by Working Group III of the of the Intergovernmental Panel on Climate Change. Metz, B., Davidson, O. de Coninck, H.C., Loos, M. & Meyer, L.A. (ur.). CambridgeUniversity Press, Cambridge, UK.

IPCC (2014): Climate Change 2014: Synthesis Report. Contribution of Working Groups I, II and III to the Fifth Assessment Report of the Intergovernmental Panel on Climate

Change [Core Writing Team, R.K. Pachauri and L.A. Meyer (eds.)]. IPCC, Geneva, Switzerland, 151 pp.

KOLENKOVIĆ, I. (2012): Mogućnosti za geološko skladištenje ugljičnoga dioksida u gornjomiocenskim pješčenjacima zapadnog dijela Savske depresije. Disertacija, Rudarsko-geološko-naftnifakultet Sveučilišta u Zagrebu, 130 str.

LIEBSCHER A, MÖLLER F, BANNACH A, KÖHLER S, WIEBACH J, SCHMIDT-HATTENBERGER C, WEINER M, PRETSCHNER C, EBERT K,ZEMKE J. (2013): Injection operation and operational pressure-temperature monitoring at the CO_2 storage pilot site Ketzin, Germany - Design, results, recommendations. Int J Greenhouse Gas Control; 15: 163-173.doi:10.1016/j.ijggc.2013.02.019.

MÖLLER F., MARTENS S., LIEBSCHER A., STREIBEL M.(2015): Dataset of the back-production test at the CO_2 storage pilot site Ketzin, Germany. Scientific Technical Report: Data ; 15/03, Potsdam, 6 p., doi: 10.2312/GFZ.b103-15037

NORDEN B, FÖRSTER A, VU-HOANG D, MARCELIS F, SPRINGER N, LE NI I (2010): Lithological and petrophysical core-log interpretation in CO2SINK, the European CO_2 onshore research storage and verification project. SPE Reserv Eval Eng 13(2):179–192. doi: 10.2118/115247-PA.

NORDEN B., FRYKMAN P. (2013): Geological modelling of the Triassic Stuttgart Formation at the Ketzin CO_2 storage site, Germany; International Journal of Greenhouse Gas Control 19; doi: 10.1016/j.ijggc.2013.04.019

PARKHURST, D.L., APPELO, C.A.J.(1999): User's guide to PHREEQC (version 3)-A computer 737 program for speciation, batch-reaction, one-dimensional transport, and inverse geochemical 738 calculations. U.S. Geological Survey Water-Resources Investigations Report 99–4259.

PARKHURST, D.L., APPELO C.A.J. (2012): Description of Input and Examples for PHREEQC Version 3—A Computer Program for Speciation, Batch-Reaction, One-Dimensional Transport, and Inverse Geochemical Calculations, Chapter 43 of Section A, Groundwater Book 6, Modeling Techniques, Techniques and Methods 6–A43,U.S. Geological Survey, Denver.

PEREŠIN, D. (2011): Regionalna procjena kapaciteta skladištenja ugljičnog dioksida u gornjomiocenskim pješčenjacima zapadnog dijela Savske depresije. Diplomski rad, RGN fakultet Sveučilišta u Zagrebu, 34. str.

RISEK, M. (2013); Kartiranje prostornog rasporeda poroznosti u svrhu procjene kapaciteta geološkog uskladištenja ugljičnig dioksida. Diplomski rad, RGN fakultet Sveučilišta u Zagrebu, 45. str.

SAFTIĆ, B. (1993): Taložni sustav pješčanih rezervoara genetske sekvencije slojeva pješčenjaka Poljana u neogenskim naslagama polja Žutica. Magistarski rad. Rudarsko-geološko-naftni i Prirodoslovno-matematički fakultet Sveučilišta u Zagrebu, Zagreb, 55 str.

SAFTIĆ, B., VELIĆ, J., ŠIMON, J. & NOVAK, J. (1995): High-resolution Palaeogeographic Maps of Sandstone Reservoirs: GSS Poljana (Pontian), Žutica Oil & Gas Field, Sava Depression.- in VLAHOVIĆ et al. eds.: First Croatian Geological Congress, Opatija 18-21.10.1995., Proceedings 2, 529-533, Zagreb 1995.

SAFTIĆ, B. (1998): Genetska stratigrafska sekvencijska snaliza pontskih naslaga u zapadnom dijelu Savske depresije. Disertacija, Rudarsko-geološko-naftni fakultet Sveučilišta u Zagrebu, 136 str.

SAFTIĆ, B., KOLENKOVIĆ, I., VULIN, D. (2008): Putting carbon dioxide back in the subsurface - possibilities in Croatia.- in: Franković, B. (ed.): Energija i okoliš 2008/ Energy and Environment 2008., Hrvatski savez za sunčevu energiju, 79-88.

SAFTIĆ,B, TOMLJENOVIĆ I., KREŠIĆ D,., RISEK M. (2015): Porosity distribution models for numerical estimates of the regional CO_2 storage potential in clastic sediments; 7^{th} HR-HU Geomathematical congress, Morahalom, Hungary, 175p.

SCHILLING, F., BORM, G., WÜRDEMANN, H., MÖLLER, F., KÜHN, M., AND THE CO2SINK GROUP (2009): Status Report on the First European on-shore CO_2 Storage Site at Ketzin (Germany). Energy Procedia, 1, 1, 2029-2035.

SPAN, R., WAGNER, W. (1996): A new equation of state for carbon dioxide covering the flu id region from the triplepoint temperature to 1100K at pressures up to 800 MPa. J. Phys.Chem. Ref. Data 25, 1509–1596.

SAYLOR, B., ZERAI, B. (2004): Injection and Trapping of CO_2 in Deep Saline Aquifer: In: Giere R. and Stille P. (eds): Energy, Waste, and the Environment: A Geochemical Approach. Geological Society of London, 285-296 p.

STUMM, W., MORGAN J. (1996): Aquatic chemistry: chemical equilibria and rates in natural waters, 3rd edition, A Wiley-Interscience publication, New York, 1022 p.

TADEJ, J& KRIZMANIĆ, K. (1995): Paleoecology and Depositional Environments of the Upper Miocene Sediments in the NW Part of the Sava Depression, First Croatian Geological Congress, Opatija 18-21.10.1995., Proceedings, 2, 605-608, Zagreb.

TADEJ, J., MARIĆ-ĐUREKOVIĆ, Ž. & SLAVKOVIĆ, R. (1996): Porosity, Cementation, Diagenesis and Their Influence on the Productive Capability of Sandstone Reservoirs in the Sava Depression (Croatia). U: Velić, J., Hernitz, Z. & Saftić, B. (ur.): Proceedings of the 1st International Symposium of Petroleum Geology, Zagreb, April 18-19, 1996., Geologia Croatica, 49/2, 311-316.

VULIN, D. (2010): Modeliranje termodinamičkih i petrofizičkih parametara za geološko skladištenje ugljičnog dioksida. Disertacija. Rudarsko-geološko-naftni fakultet Sveučilišta u Zagrebu, 120 str., Zagreb.

WIESE B, NIMTZ M, MÖLLER F, OTTO C, KÜHN M, LIEBSCHER A, SCHMIDT-HATTENBERGER C. (2012): Determination of thermodynamics in a CO_2 injection well using pressure and distributed temperature sensing. IAHS Redbook; 355: 286-290.

WIESE B, ZIMMER M, NOWAK M, PELLIZZARI L, PILZ P. (2013): Well-based hydraulic and geochemical monitoring of the above zone of the CO_2 reservoir at Ketzin, Germany. Env Earth Sci; 70; 3709-3726. doi: 10.1007/s12665-013-2744.

WOLERY T.W., JAREK R.L.(2003): Civilian Radioactive Waste Management System Management & Operating Contractor SOFTWARE USER'S MANUAL EQ3/6, Version 8.0, Sandia National Laboratories P.O. Box 5800 Albuquerque, New Mexico.

10.2 Archived documents

ŠIMON, J. (1963*): Litostratigrafske jedinice polja IvanićGrad. Fond struč. dokum. INA Industrija nafte d.d., Zagreb.

ŠIMON, J. (1964*): Litostratigrafske jedinice polja Kloštar Ivanić. Fond struč. dokum. INA Industrija nafte d.d., Zagreb.

ŠIMON, J. & DOMBOVIĆ, D. (1965*): Litostratigrafske jedinice Zagrebačke zone. Fond struč. dokum. INA – Industrija nafte d.d., Zagreb.

10.3 Web sources

www.co2geonet.com (http://online.fliphtml5.com/iomp/mtiw/)

http://www.CO2ketzin.de/

www.umich.edu/~chem241/lecture11final.pdf

http://wwwbrr.cr.usgs.gov/projects/GWC_coupled/phreeqc/faq.html

http://mineral.gly.bris.ac.uk/AqueousGeochemistry

http://wwwbrr.cr.usgs.gov/projects/GWC_coupled/phreeqc/html/final-4.html

http://www.aqion.de/site/92

http://statistics.about.com/

http://sociology.about.com/od/Statistics/a/Linear-Regression-Analysis.htm

http://mathbits.com/MathBits/TISection/Statistics2/correlation.htm

http://www.chem1.com/acad/pdf/c3carb.pdf

https://skepticalscience.com/print.php?n=888

Appendix 1 *NCSS multiple regression analysis*

Dependent variable: Measured Porosity (well-logging)

Predicted porosities:

Row	Actual Measured Porosity	Predicted porosity	Standard Error of Predicted	Y Coordinate Axis	X Coordinate Axis
An-1	15	17.7	2.8	5603101	5074916
2		17.6	2.8	5601074	5077418
3		17.6	2.8	5600736	5076723
BS-1	21	18.4	2.9	5600115	5077402
5		16.4	2.8	5592718	5076313
6		16.5	2.9	5593564	5076878
7		15.1	2.6	5604484	5059990
8		16.1	2.9	5589484	5078073
D-2	21	16.1	2.7	5589916	5077151
10		15	2.7	5600816	5064361
11		15.4	2.6	5601815	5064900
12		16.2	2.7	5598518	5075959
13		17	2.9	5595128	5079523
14		16.8	2.7	5597595	5075352
15		17.2	2.9	5596456	5075885
16		17.2	2.8	5596154	5075790
17		16.1	2.9	5610345	5052831
18		14.5	2.7	5611491	5050474
GOS-3	14	15.3	2.7	5610520	5051630
20		13.7	2.9	5614533	5056988
21		15.1	2.7	5606898	5062516
22		15.3	2.7	5608002	5063818
23		16.4	2.8	5609117	5059066
24		14.5	2.8	5609380	5059985
Je-1DU	16	15.1	2.7	5602540	5065110
26		15.4	2.6	5603109	5056009
27		15.2	2.6	5601590	5065830
28		15.4	2.6	5603041	5064603
29		15.4	2.6	5601786	5066700
30		15.4	2.6	5601181	5066675
31		15.1	2.7	5602100	5065450
32		16.9	2.9	5610757	5067328
33		16.4	2.8	5609416	5067912
34		17.1	2.9	5611761	5068443
35		15.6	2.9	5608683	5066314
36		15.9	2.8	5608514	5067000
37		18.2	2.9	5601400	5078345
38		15.7	2.6	5606250	5072600

Wells	Actual Measured Porosity	Predicted porosity	Standard Error of Predicted	Y Coordinate Axis	X Coordinate Axis
39		17.4	2.8	5605833	5071094
40		17.5	2.8	5605260	5071624
Lup-8	17	17.4	2.7	5605797	5070442
42		15.2	2.6	5599896	5069019
43		15.3	2.6	5600439	5069244
Obo-1	17	16	2.9	5597650	5061850
45		15.8	2.8	5596250	5061910
Od-1	14	13.9	2.7	5591970	5066594
Ok-1DU	12	14.3	2.7	5617450	5051586
48		14.7	2.6	5618419	5050669
49		13.5	2.8	5620644	5051899
50		13.8	2.7	5619235	5051233
51		14.7	2.6	5617277	5050810
52		15.9	2.6	5605459	5065544
Pre-2	19	16.3	2.6	5603073	5069382
54		16.1	2.9	5596475	5062620
55		15.2	2.7	5606397	5061674
PB-3 alfa	14	15.1	2.6	5605783	5060824
Pč-2	14	15.4	2.7	5600760	5058680
58		15.9	2.9	5596263	5067954
59		16.3	3.1	5593860	5068684
Ru-3	15	15.9	2.8	5596930	5068760
Rv-1	18	14.3	2.7	5611601	5059245
62		16.4	2.7	5587586	5077188
63		16.8	2.9	5586733	5078639
64		17.1	2.8	5599540	5079361
Št-1JU	13	17.4	3	5600120	5080585
Vel-1	12	14	2.7	5597246	5057473
Vl-2	13	13.6	2.8	5623279	5050930
68		17.4	2.7	5605575	5077524
69		14	2.8	5616684	5054479
70		14.3	2.7	5617496	5053852
71		14.2	2.8	5613439	5053632
72		15.5	2.7	5608344	5056275
73		14.5	2.7	5614260	5053332
74		14.7	2.7	5613378	5055426
75		15.5	2.6	5611293	5056708
76		14.7	2.7	5611478	5054832
Žu-249DU	16	14.8	2.7	5613511	5054169
78		14.5	2.7	5613390	5056790

***Appendix 2** Žu-249 – Water chemistry*

Water analysis INA d.d.	Sampling	03.01.2014.		09.10.2014	
	Anaylsis	17.01.2014		15.10.2014.	
CATIONS	*mg/l*		*%ekv*	*mg/l*	*%ekv*
NH_4^+	43.48		0.217	51.96	0.228
Na^+	12000		46.935	11200	38.617
K^+	299.5		0.689	4255	8.627
Mg_2^+	40.4		0.299	64.9	0.423
Ca_2^+	379		1.701	427.7	1.692
Sr_2^+	124.6		0.256	195.2	0.352
Fe (total)	128			37.6	
Fe^{2+}				30.05	0.085
ANIONS					
Cl^-	18896.4		47.927	21803.6	48.750
HCO_3^-	819.09		1.207	727.32	0.945
SO_4^{2-}	411.6		0.771	169.2	0.279
TDS as mg/l NaCl	30900			33004	
Dissolved gasses					
H_2S	no data			1.56	
CO_2	no data			385	
Texture	Muddy			muddy, oil traces	
Colour	Brown			yellowish-grey	
Odour	hydrocarbons and chemicals			hydrocarbons	

Appendix 3 *Percent errors in charge balance – Žu-246*

PERCENT ERROR IN CHARGE BALANCE				**Žu-246**	**3.01.2014.**
cations	*mg/l*	*Mr*	*mmol/l*	*Charge*	*meq/l*
NH_4^+	**43.48**	18.04	2.4102	1	2.4102
Na^+	**12000**	22.99	521.9661	1	521.9661
K^+	**2999.5**	39.1	76.71355	1	76.71355
Mg^{2+}	**40.4**	24.3	1.662551	2	3.325103
Ca^{2+}	**379**	40.08	9.456088	2	18.91218
Sr^{2+}	**124.6**	87.62	1.42205	2	2.8441
Fe^{2+}	**120**	55.84	2.148997	2	4.297994
Fe^{3+}	**8**	55.84	0.538154	3	1.614462
anions				**SUM**	**632.0837**
Cl^-	**18896.4**	35.45	533.0437	-1	-533.044
HCO_3^-	**819.09**	61.019	13.42352	-1	-13.4235
SO_4^{2-}	**411.6**	96.06	4.284822	-2	-8.56964
				SUM	**-555.037**
RESULT =	$(100\frac{cations - \lvert anions \rvert}{cations + \lvert anions \rvert})$				**6.49**

PERCENT ERROE IN CHARGE BALANCE				**Žu-246**	**15.10.2014.**
cations	mg/l	Mr	mmol/l	Charge	meq/l
NH_4^+	**51.96**	18.04	2.880266	1	2.880266
Na^+	**11200**	22.99	487.1683	1	487.1683
K^+	**4255**	39.1	108.8235	1	108.8235
Mg^{2+}	**64.9**	24.3	2.670782	2	5.341564
Ca^{2+}	**427.7**	40.08	10.67116	2	21.34232
Sr^{2+}	**195.2**	87.62	2.227802	2	4.455604
Fe^{2+}	**30.05**	55.84	0.538145	2	1.076289
Fe^{3+}	**7.6**	55.84	0.538154	3	1.614462
anions				**SUM**	**632.7024**
Cl^-	**21803.6**	35.45	615.0522	-1	-615.052
HCO_3^-	**727.32**	61.019	11.91957	-1	-11.9196
SO_4^{2-}	**169.2**	96.06	1.761399	-2	-3.5228
				SUM	**-630.495**
RESULT	$(100\frac{cations - \lvert anions \rvert}{cations + \lvert anions \rvert})$				**0.17478**

Appendix 4 *Žutica 249 – PHREEQC simulation*

```
DATABASE C:\phreeqc\database\pitzer.dat   #2.Simulation – phreeqc.dat
TITLE Zu249
SOLUTION 1 15.10.2014.
 temp      25. # water temperature measured on the surface
 units     mg/l
 density   1.0232     # of solution
 pH        6.8
 Na        11200  #
 K         4255
 Cl        21803.6 charge #without charge is also correct
 Ca        427.7
 Mg        64.9
 S(6)         169.2    as SO4
 Alkalinity  727.32 as HCO3
 Fe        37.6
 Sr        195.2
END
USE solution 1
REACTION_PRESSURE 1
165
REACTION_TEMPERATURE 1
83 # Celsius degrees
END
USE solution 1
USE reaction_temperature 1
EQUILIBRIUM_PHASE 1
CO2(g) 2.2116 #log of 162.8 atm
END
```

Appendix 5 *Ketzin – PHREEQC simulation – First day of back-production test*

```
DATABASE C:\phreeqc\database\pitzer.dat
TITLE PWU and GFZ analysis of the brine at Ketzin during the back-production test
SOLUTION 1  16.10.14 11:15 (1st day)
 temp      19.0 # water temperature measured on the surface
 units     mg/l
 density   1.15        #solution
 water     1.
 pH        6.0
 Na        85068.
 K         834.
 Cl        141396. charge
 Ca        2042.
 Mg        951.
 S(6)      4420.      as SO4
 Alkalinity           2423.1  as HCO3 # molality --> 4.336e-02
 Fe        371.
 Mn        2.389
 Sr        52.
 Si        100.
#REACTION_PRESSURE 1
#GAS_PHASE 1
#-fixed_pressure
#-pressure
#-volume
#-temperature 19
#CO2(g)  # using SAVE solution 2, the result is the same
END
USE solution 1
REACTION_TEMPERATURE 1
  34 # Celsius degrees
END
USE solution 1
REACTION_PRESSURE 1 #not necessary if pressure is defined as gas_phase with fixed pressure
64.64
REACTION_TEMPERATURE 1
  34 # Celsius degrees
EQUILIBRIUM_PHASE 1
CO2(g) 1.81 # log of 64.64 atm
END
```

Appendix 6 *Ketzin – PHREEQC – The last day of back-production test*

```
DATABASE C:\phreeqc\database\pitzer.dat
TITLE PWU and GFZ analysis of brine
SOLUTION 1 Solution 27.10.14 10:30
 temp      21.0 # water temperature measured on the surface
 units     mg/l
 density   1.15        #solution
 pH        6.23
 Na        85504.
 K         869.
 Cl        136956. charge
 Ca        2061.
 Mg        953.
 S(6)          4308.       as SO4
 Alkalinity  2147.9  as HCO3
 Fe        307.
 Mn        2.302
 Sr        50.
 Si        100.
END
USE solution 1
REACTION_PRESSURE 1
64.64
REACTION_TEMPERATURE 1
  34 # Celsius degrees
EQUILIBRIUM_PHASE 1
CO2(g) 1.81
END
USER_GRAPH 1 # to run user graph, copy all input except database
       -headings Temperature CO2(g) Calcite Anhydrite
       -chart_title "CO2(g)-Calcite-Anhydrite Stability"
       -axis_scale x_axis #automatic if not specified
       -axis_scale y_axis
       -axis_titles "Temperature,°C" "Saturation index"
       -initial_solutions true
  -start
  10 graph_x TC
  20 graph_y SI("CO2(g)")SI("Calcite")SI("Anhydrite")
  # 30 third (right axis)
  -end
END
```

Appendix 7 *Ketzin – PHREEQC simulation – Pre-injection data*

```
DATABASE C:\phreeqc\database\pitzer.dat
TITLE Initial solution # pre-injection test
SOLUTION 1 Average value from 3 days excluding first day
# data from the first day is not used because the concentrations are quite different(impurities)
 temp      20. # water temperature measured on the surface
 units     mg/l
 density   1.151
 pH        6.5
 Na        89733.33
 K         291.
 Cl        138000. charge
 Ca        2094.
 Mg        843.
 S(6)      3686.      as SO4
 Alkalinity        57.        as HCO3
 Fe        6.22
 Mn        1.4
 Sr        48.43
 #Zn
 Si        9.33    as H4SiO4
 #Li       1.8
 #Ba       0.07
 #Br       45.47
 #B        35.87    as B(OH)3
END
USE solution 1
REACTION_TEMPERATURE 1
  34
REACTION_PRESSURE 1
64.64 #initial reservoir pressure
END
```

Appendix 8 *Chemical formulas of some minerals from the simulation*

Anhydrite	CaSO4	**Kalicinite**	KHCO3
Aragonite	CaCO3	**Magnesite**	MgCO3
Calcite	CaCO3	**Nahcolite**	NaHCO3
Celestite	SrSO4	**Sylvite**	KCl
Dolomite	CaMg(CO3)2	**Thenardite**	Na2SO4
Glauberite	Na2Ca(SO4)2	**Goethite**	FeOOH
Goergeyite	K2Ca5(SO4)6H2O	**Hematite**	Fe2O3
Gypsum	CaSO4:2H2O	**Sylvite**	SrCO3
Halite	NaCl	**Magnetite**	Fe3O4
Maghemite	Fe2O3		